

DUDLEY KNOX LIBRARY
NAVAL POSTGRADUATE SCHOOL
MONTEREY CA 93943-5101

DUDLEY KNOX LIBRARY
NAVAL POSTGRADUATE SCHOOL
MONTEREY CA 93943-5101

Approved for public release; distribution is unlimited.

**Design of Robust Suboptimal Controllers for a Generalized Quadratic
Criterion**

by

**Kurtis Brett Miller
Lieutenant, United States Navy
B.S., Colorado State University, 1986**

Submitted in partial fulfillment of the requirements for
the degree of

MASTER OF SCIENCE IN ELECTRICAL ENGINEERING

from the

**NAVAL POSTGRADUATE SCHOOL
June 1992**

Computer Engineering

REPORT DOCUMENTATION PAGE

Form Approved
OMB No. 0704-0188

REPORT SECURITY CLASSIFICATION Unclassified		1b. RESTRICTIVE MARKINGS	
SECURITY CLASSIFICATION AUTHORITY		3. DISTRIBUTION/AVAILABILITY OF REPORT Approved for public release; distribution is unlimited.	
DECLASSIFICATION/DOWNGRADING SCHEDULE			
PERFORMING ORGANIZATION REPORT NUMBER(S)		5. MONITORING ORGANIZATION REPORT NUMBER(S)	
NAME OF PERFORMING ORGANIZATION Naval Postgraduate School	6b. OFFICE SYMBOL (If applicable) 33	7a. NAME OF MONITORING ORGANIZATION Naval Postgraduate School	
ADDRESS (City, State, and ZIP Code) Monterey, CA 93943-5000		7b. ADDRESS (City, State, and ZIP Code) Monterey, CA 93943-5000	
NAME OF FUNDING/SPONSORING ORGANIZATION	8b. OFFICE SYMBOL (If applicable)	9. PROCUREMENT INSTRUMENT IDENTIFICATION NUMBER	
ADDRESS (City, State, and ZIP Code)		10. SOURCE OF FUNDING NUMBERS	
		PROGRAM ELEMENT NO.	PROJECT NO.
		TASK NO.	WORK UNIT ACCESSION NO.

TITLE (Include Security Classification)
DESIGN OF ROBUST SUBOPTIMAL CONTROLLERS FOR A GENERALIZED QUADRATIC CRITERION

PERSONAL AUTHOR(S)
Kurtis B. Miller

TYPE OF REPORT Master's Thesis	13b. TIME COVERED FROM _____ TO _____	14. DATE OF REPORT (Year,Month,Day) June 1992	15. PAGE COUNT 66
--	--	---	-----------------------------

SUPPLEMENTARY NOTATION
The views expressed in this thesis are those of the author and do not reflect the official policy or position of the Department of Defense or the U.S. Government.

COSATI CODES			18. SUBJECT TERMS (Continue on reverse if necessary and identify by block number) Linear Quadratic Feedback Control System, Robust Control, Optimal Control, Suboptimal Control
FIELD	GROUP	SUB-GROUP	

ABSTRACT (Continue on reverse if necessary and identify by block number)

Standard linear quadratic regulator (LQR) designs guarantee a certain level of robustness. However, optimizing a generalized quadratic criterion produces coupled state and input terms and there are no longer any guarantees of good robustness properties. This thesis identifies how this problem arises and then presents several suboptimal, but robust controller design options which provide the control systems engineer with the ability to perform a trade-off between performance and robustness. The effectiveness of these methods is investigated and the trade-offs between performance and robustness are evaluated using computer simulation of a statically unstable fighter aircraft.

DISTRIBUTION/AVAILABILITY OF ABSTRACT <input checked="" type="checkbox"/> UNCLASSIFIED/UNLIMITED <input type="checkbox"/> SAME AS RPT. <input type="checkbox"/> DTIC USERS		21. ABSTRACT SECURITY CLASSIFICATION Unclassified	
2. NAME OF RESPONSIBLE INDIVIDUAL Won-Zon Chen		22b. TELEPHONE (Include Area Code) (408) 646 - 2928	22c. OFFICE SYMBOL EC/Cw

ABSTRACT

Standard linear quadratic regulator (LQR) designs guarantee a certain level of robustness. However, optimizing a generalized quadratic criterion produces coupled state and input terms and there are no longer any guarantees of good robustness properties. This thesis identifies how this problem arises and then presents several suboptimal, but robust controller design options which provide the control systems engineer with the ability to perform a trade-off between performance and robustness. The effectiveness of these methods is investigated and the trade-offs between performance and robustness are evaluated using computer simulation of a statically unstable fighter aircraft.

TABLE OF CONTENTS

I. INTRODUCTION.....	1
II. BACKGROUND LINEAR QUADRATIC THEORY.....	3
A. STANDARD LINEAR QUADRATIC CONTROL THEORY	3
B. ROBUSTNESS PROPERTIES OF LQ DESIGNS	5
C. THE GENERALIZED QUADRATIC CRITERION	8
D. ROBUSTNESS FOR A GENERALIZED QUADRATIC CRITERION	12
III. MODEL UNCERTAINTY AND ROBUSTNESS MEASURES FOR MULTIVARIABLE SYSTEMS.....	15
A. MODEL UNCERTAINTY FOR MIMO SYSTEMS	15
B. ROBUSTNESS MEASURES FOR MIMO SYSTEMS	17
1. Principal Region	17
2. Minimum Singular Value	19
IV. ROBUST SUBOPTIMAL DESIGN.....	22
A. ROBUSTNESS DESIGN OPTIONS	22
1. Option I: $\tilde{S} = 0$	23
2. Option II: $\tilde{Q} = Q + SS^*$, $\tilde{R} = R + I$	23
3. Option III: $\tilde{R} = \rho R$	23
4. Option IV: $\tilde{S} = \rho S$, $\rho \leq 1$	24
5. Option V: $\tilde{R} = \rho R$, $\tilde{Q} = Q + (\rho - 1)SR^{-1}S^*$, $\rho \geq 1$	24
6. Option VI: $\tilde{Q} = \rho Q$	25
7. Option VII: $\tilde{Q} = Q + \rho SR^{-1}S^*$, $\rho \geq 1$	26
V. A NUMERICAL EXAMPLE AND SIMULATION.....	27
A. STATICALLY UNSTABLE AIRCRAFT MODEL	27

B. SIMULATIONS	33
1. Optimal System	34
2. System with $\tilde{Q} = Q + SS^*$, $\tilde{R} = R + I$	36
3. System with $\tilde{R} = \rho R$	38
4. System with $\tilde{S} = \rho S$, $\rho \leq 1$	39
5. System with $\tilde{R} = \rho R$, $\tilde{Q} = Q + (\rho - 1)SR^{-1}S^*$, $\rho \geq 1$	42
6. System with $\tilde{Q} = \rho Q$	45
7. System with $\tilde{Q} = Q + \rho SR^{-1}S^*$, $\rho \geq 1$	48
C. FURTHER INVESTIGATION OF OPTION IV	51
VI. CONCLUSION.....	54
REFERENCES.....	56
INITIAL DISTRIBUTION LIST.....	57

LIST OF FIGURES

Figure 2.1	Closed-Loop Linear System	4
Figure 2.2	Definitions of Robustness Measures [After Ref. 3]	6
Figure 2.3	Robustness of an LQ System [After Ref. 3]	8
Figure 3.1	System with Unstructured Uncertainties	17
Figure 3.2	Principal Region and Stability Margins for MIMO systems [After Ref. 4]	18
Figure 5.1	Pitch Pointing, Constant Flight Path	28
Figure 5.2	Direct Lifting, Constant Pitch	28
Figure 5.3	Definitions of State Variables α , θ , and q	29
Figure 5.4	Wind Gust Disturbance Inputs	33
Figure 5.5	Angle of Attack	33
Figure 5.6	Minimum Singular Values of the Optimal System	34
Figure 5.7	Response of the Optimal System to a Rectangular Gust	35
Figure 5.8	Response of the Optimal System to a Triangular Gust	35
Figure 5.9	Minimum Singular Values Using $\tilde{\mathbf{Q}} = \mathbf{Q} + \mathbf{S}\mathbf{S}^*$, $\tilde{\mathbf{R}} = \mathbf{R} + \mathbf{I}$	36
Figure 5.10	Square Gust Response of $\tilde{\mathbf{Q}} = \mathbf{Q} + \mathbf{S}\mathbf{S}^*$, $\tilde{\mathbf{R}} = \mathbf{R} + \mathbf{I}$	37
Figure 5.11	Triangular Gust Response of $\tilde{\mathbf{Q}} = \mathbf{Q} + \mathbf{S}\mathbf{S}^*$, $\tilde{\mathbf{R}} = \mathbf{R} + \mathbf{I}$	37
Figure 5.12	Performance vs ρ for $\tilde{\mathbf{R}} = \rho\mathbf{R}$	38
Figure 5.13	Robustness vs ρ for $\tilde{\mathbf{R}} = \rho\mathbf{R}$	38
Figure 5.14	Performance vs ρ for $\tilde{\mathbf{S}} = \rho\mathbf{S}$, $\rho \leq 1$	39
Figure 5.15	Robustness vs ρ for $\tilde{\mathbf{S}} = \rho\mathbf{S}$, $\rho \leq 1$	39

Figure 5.16 Square Gust Response for $\tilde{S} = \rho S$, $\rho \leq 1$	40
Figure 5.17 Triangular Gust Response for $\tilde{S} = \rho S$, $\rho \leq 1$	41
Figure 5.18 Performance vs ρ for $\tilde{R} = \rho R$, $\tilde{Q} = Q + (\rho - 1)SR^{-1}S^*$, $\rho \geq 1$	42
Figure 5.19 Robustness vs ρ for $\tilde{R} = \rho R$, $\tilde{Q} = Q + (\rho - 1)SR^{-1}S^*$, $\rho \geq 1$	42
Figure 5.20 Rectangular Gust Response for $\tilde{R} = \rho R$, $\tilde{Q} = Q + (\rho - 1)SR^{-1}S^*$, $\rho \geq 1$	43
Figure 5.21 Triangular Gust Response for $\tilde{R} = \rho R$, $\tilde{Q} = Q + (\rho - 1)SR^{-1}S^*$, $\rho \geq 1$	44
Figure 5.22 Performance vs ρ for $\tilde{Q} = \rho Q$	45
Figure 5.23 Robustness vs ρ for $\tilde{Q} = \rho Q$	45
Figure 5.24 Square Gust Response for $\tilde{Q} = \rho Q$	46
Figure 5.25 Triangular Gust Response for $\tilde{Q} = \rho Q$	47
Figure 5.26 Performance vs ρ for $\tilde{Q} = Q + \rho SR^{-1}S^*$, $\rho \geq 1$	48
Figure 5.27 Robustness vs ρ for $\tilde{Q} = Q + \rho SR^{-1}S^*$, $\rho \geq 1$	48
Figure 5.28 Square Gust Response for $\tilde{Q} = Q + \rho SR^{-1}S^*$, $\rho \geq 1$	49
Figure 5.29 Triangular Gust Response for $\tilde{Q} = Q + \rho SR^{-1}S^*$, $\rho \geq 1$	50
Figure 5.30 Frequency Shaping as a Function of ρ	53

ACKNOWLEDGMENTS

I would first like to acknowledge Prof. Won-Zon Chen for giving me the opportunity to do this thesis and to work with him. His time, assistance, encouragement, and patience were invaluable. His insight and experience with mathematics and control systems has inspired me to continue in this field and for that I'll be forever grateful.

My most heartfelt gratitude goes to my wife, Liz, who never complained when I was preoccupied with studies or away due to many late nights and long hours in the lab. Her continual love, support, and encouragement helped to make my time at NPS a positive experience.

I. INTRODUCTION

Modern weapons systems are becoming more and more complex and are constantly pushing the limits of technology. Performance, in terms of agility and faster response, are demanded at the same time that reliability and operation in a wider variety of environments and applications are required. All of this highlights the importance of the design of the underlying control systems of the weapon.

Many times a choice must be made as to the minimum level of reliability or robustness acceptable at the expense of a certain amount of performance. For a single-input single-output (SISO) linear quadratic optimal control system in which there is no cross-coupling of the states of the system and the control inputs, there are well defined and guaranteed levels of robustness. However, for a multivariable or multi-input multi-output (MIMO) system, while the guarantees still apply, the measurement of the robustness of a system is not necessarily well defined. In addition, for a system with cross-coupling of the states and inputs, which can occur when the performance measure is in the generalized quadratic form, there are no longer any guarantees on the robustness. An optimized system of this type may be vulnerable to even minor uncertainties or deviations from the model used to design the control system.

Design techniques do exist for working with these problems, but they are typically of a graphical nature and do not easily provide a way to measure and vary the trade-off between performance and robustness. The goal of this thesis then is to develop a design method for using one variable parameter to quickly and easily get a measure of this trade-off. The focus will be confined to

generalized linear quadratic, finite-dimensional, multi-input multi-output systems. It is assumed that full state feedback is available so observers will not be necessary. In addition, measurement and plant noise will be ignored for this development, so techniques such as Kalman filtering will not be necessary. After developing several methods for designing suboptimal robust controllers, these will be simulated using a statically unstable fighter aircraft which provides a convenient MIMO model. Also, the required performance will be chosen such that the cross-coupling of the states and the control inputs will occur.

II. BACKGROUND LINEAR QUADRATIC THEORY

Standard linear quadratic (LQ) control theory is well understood and many tools exist for designing these systems. As long as the states and the inputs are not coupled in the performance function, these systems have very good and well defined properties of stability and robustness. However, when there is a coupling between the states and the control inputs, the robustness of the system is no longer guaranteed. This chapter presents a quick review of the pertinent aspects of the standard theory, points out where and how the cross coupling of the states and inputs occurs, and the problems this creates.

A. STANDARD LINEAR QUADRATIC CONTROL THEORY

A linear finite-dimensional time-invariant dynamic system can be described in a compact form by input and output equations

$$\dot{x} = Ax + Bu, \quad (2-1)$$

and

$$y = Cx, \quad (2-2)$$

where x is an $n \times 1$ state vector, u is an $m \times 1$ control input vector, y is a $p \times 1$ output vector, and A , B , C , and D are system matrices of the necessary dimensions. Feedback control laws can be used to either stabilize the system or modify its response to meet the specifications of a particular application.

Assuming that all states of the system can be measured, a feedback control law is computed as a linear combination of the states

$$u = -Kx, \quad (2-3)$$

where the feedback gain matrix K is determined from the type of problem and the method of control desired. This closed-loop system is depicted in Figure 2.1

Optimal control is a design method which computes K by minimizing a cost function (or maximizing a performance function). The cost function is a real-

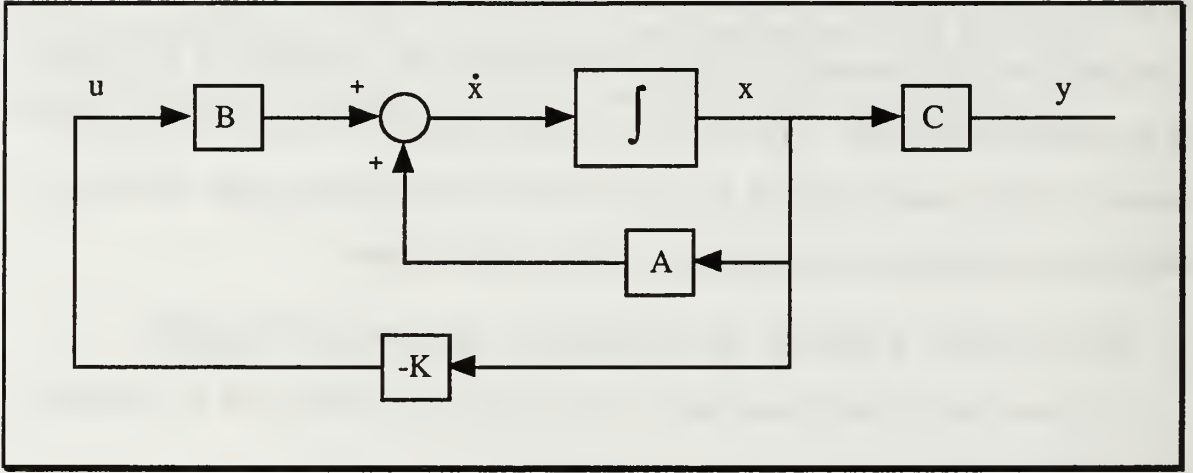


Figure 2.1 Closed-Loop Linear System

valued function of the state of the system and the control input, both of which can vary with time. Cost functions take the general form

$$J = \int_0^{\infty} f(x(t), u(t), t) dt. \quad (2-4)$$

Application of optimal control requires the specifications of the control problem of interest to be formulated in terms of an appropriate cost function. Minimum time control, terminal control, minimum control effort, minimum squared error, and combinations of these are just a few of the possibilities.

One cost function which has been found to be particularly useful is quadratic control which takes the form

$$J = \int_0^{\infty} [x^*(t)Qx(t) + u^*(t)Ru(t)]dt, \quad (2-5)$$

where $*$ denotes the complex conjugate transpose, Q is a positive semi-definite $n \times n$ matrix, and R is a positive definite $m \times m$ matrix. Kalman [Refs. 1&2] found that the optimal feedback control law for minimizing this cost function is

$$\begin{aligned} u_{opt}(t) &= -R^{-1}B^*Px_{opt}(t) \\ &= -Kx_{opt}(t), \end{aligned} \quad (2-6)$$

where $K = R^{-1}B^*P$ is determined by finding a positive definite solution P for the Steady-State Riccati Equation (SSRE),

$$PA + A^*P - PBR^{-1}B^*P + Q = 0. \quad (2-7)$$

Many algorithms are available for finding P and the feedback gain vector K . If the system is completely controllable, P is unique and the closed-loop system

$$\dot{x} = (A - BK)x \quad (2-8)$$

will be stable.

B. ROBUSTNESS PROPERTIES OF LQ DESIGNS

To design a control system, a mathematical model of the system of interest must be developed so that analytical techniques may be applied. Linear differential equations (2-1) and (2-2) comprise one such model. In addition, the model must be of a form that is accurate enough to give a *reasonable* representation of the system, yet simple enough that it leads to *practical* analytical solution techniques. Unfortunately, no useful mathematical model is capable of exactly representing a system. Usually differences will arise from

non-linearities in a system which is represented by a linear model or from the use of first or second order models as approximations of systems with higher order dynamics. In addition, parameter variations from operating conditions, environmental conditions, measurement errors, etc. may all contribute to uncertainties in the operation of the actual plant.

It is important to design a control system that can perform well over as much of the expected range of uncertainty as possible. A system that is insensitive to or tolerant of parameter variations and model uncertainties is termed *robust*. For (SISO) systems, robustness is usually measured in terms of three parameters (as depicted in Figure 2.2):

- Gain Margin -- A measure of how much the open-loop gain may be increased before the system becomes unstable.
- Gain Reduction Tolerance (GRT) -- A measure of how much the open-loop gain may be reduced before the system becomes unstable.
- Phase margin -- A measure of how much the open-loop phase delay may be increased before the system becomes unstable.

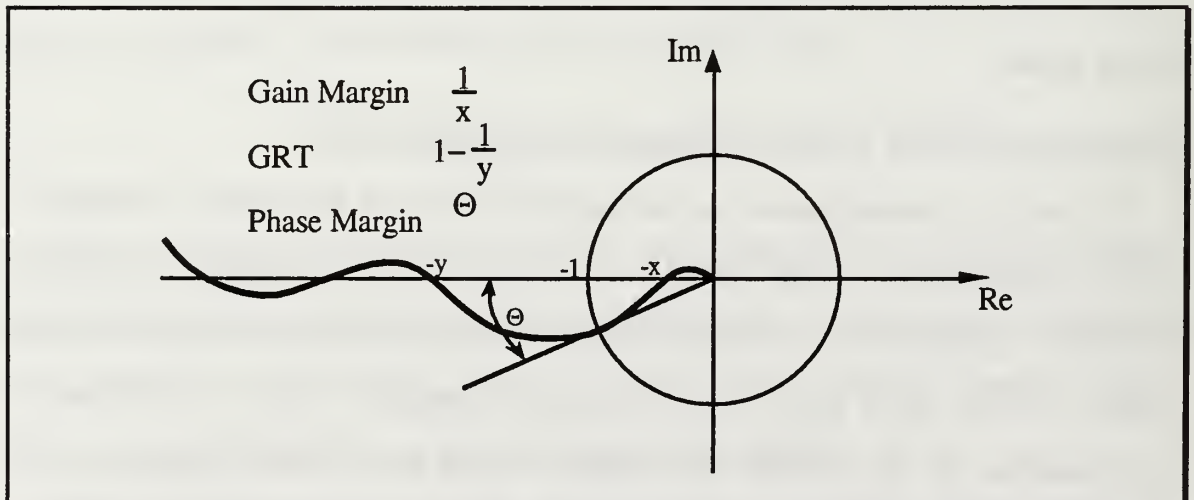


Figure 2.2 Definitions of Robustness Measures [After Ref. 3]

The optimal control system shown in Figure 2.1 has an open-loop frequency-domain transfer function

$$G(s) = (sI - A)^{-1} B, \quad s = j\omega \quad (2-9)$$

and a loop gain

$$\begin{aligned} L(s) &= KG(s) \\ &= K(sI - A)^{-1} B \\ &= R^{-1} B^* P (sI - A)^{-1} B. \end{aligned} \quad (2-10)$$

The robustness of this LQ system can be determined by algebraic manipulation of (2-7). First, add and subtract sP and then regroup terms:

$$sP - sP + PA + A^* P + Q - PBR^{-1} B^* P = 0 \quad (2-11)$$

$$-P(sI - A) - (-sI - A^*)P + Q - PBR^{-1} B^* P = 0. \quad (2-12)$$

Then multiply by $G^*(s) = B^*(-sI - A^*)^{-1}$ from the left and $G(s) = (sI - A)^{-1} B$ from the right to get

$$\begin{aligned} &-B^*(-sI - A)^{-1} PB - B^* P (sI - A)^{-1} B + B^*(-sI - A^*)^{-1} Q (sI - A)^{-1} B \\ &- B^*(-sI - A^*)^{-1} PBR^{-1} B^* P (sI - A)^{-1} B = 0 \end{aligned} \quad (2-13)$$

Noting that $B^* P (sI - A)^{-1} B = RL(s)$, (2-13) can be rewritten

$$-L^*(s)R - RL(s) + G^*(s)QG(s) - L^*(s)RL(s) = 0 \quad (2-14)$$

or

$$[I + L(s)]^* R [I + L(s)] = R + G^*(s)QG(s). \quad (2-15)$$

Since Q is positive semi-definite and $G^*(s)QG(s)$ is quadratic in $G(s)$, the right hand side of (2-15) is greater than or equal to R . Therefore, the Nyquist plot of this system must remain outside of a unit circle centered at $(-1, j0)$ as shown in Figure 2.3. The optimal linear quadratic controller is guaranteed to

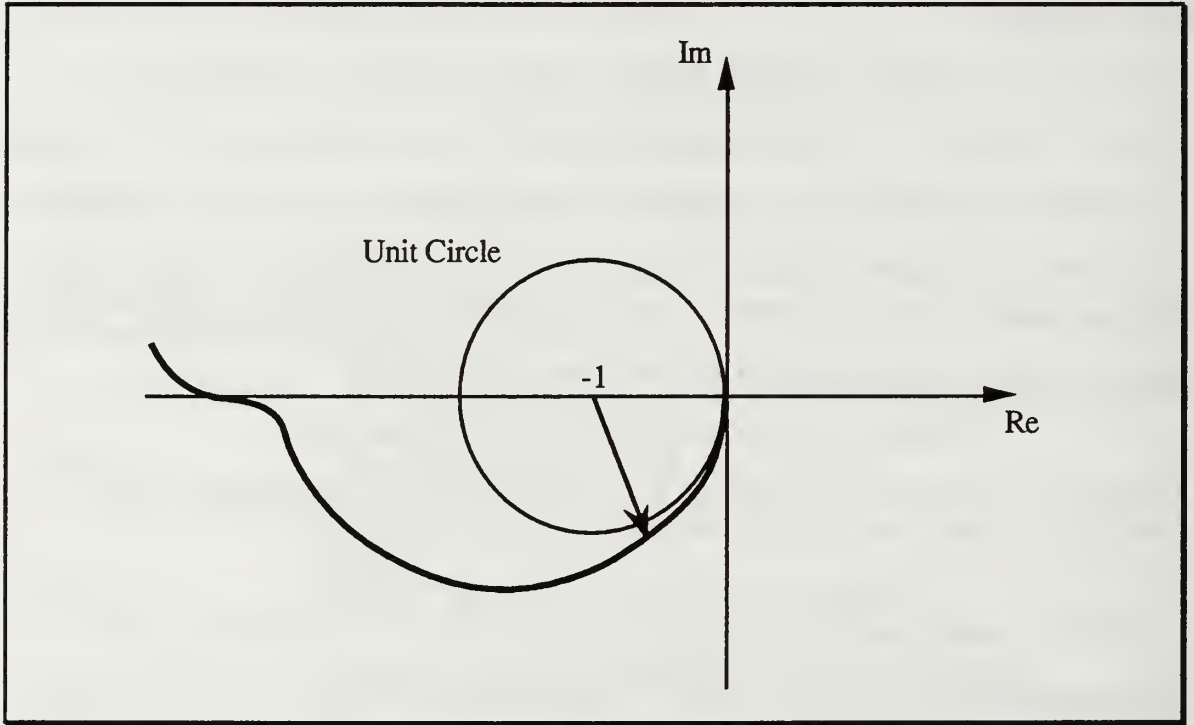


Figure 2.3 Robustness of an LQ System [After Ref. 3]

have an infinite gain margin, at least 60° of phase margin, and a minimum of 50% GRT.

C. THE GENERALIZED QUADRATIC CRITERION

A more general formulation of the quadratic control problem includes frequency shaping of the cost function. This allows frequency dependent performance requirements to be included in the system specifications. System performance can be improved, but robustness may be reduced.

A frequency shaped cost function can be generated by first transforming (2-5) into the frequency domain using Parseval's theorem,

$$J = \frac{1}{2} \int_{-\infty}^{\infty} [x^*(j\omega)Qx(j\omega) + u^*(j\omega)Ru(j\omega)]d\omega. \quad (2-16)$$

The frequency shaping is accomplished by making Q and R functions of frequency,

$$J = \frac{1}{2} \int_{-\infty}^{\infty} [x^*(j\omega)Q(j\omega)x(j\omega) + u^*(j\omega)R(j\omega)u(j\omega)]d\omega. \quad (2-17)$$

When $Q(j\omega)$ and $R(j\omega)$ meet the additional constraints that they are rational functions of $j\omega$ and decomposable into

$$Q(j\omega) = Q_1 + \Pi^*(j\omega)Q_2^* + Q_2\Pi(j\omega) + \Pi^*(j\omega)Q_3\Pi(j\omega), \quad (2-18)$$

where $\Pi(j\omega)$ is a $q \times n$ matrix of rational functions of $j\omega$ and Q_1 , Q_2 , and Q_3 are $n \times n$, $n \times q$, and $q \times q$, constant matrices respectively, an optimal controller can be obtained for this cost function by augmenting the plant to eliminate the frequency dependance of the weighting matrices and then applying standard LQ procedures. [Ref. 4]

The augmentation is accomplished by first defining

$$\tilde{x}(j\omega) = \Pi(j\omega)x(j\omega) \quad (2-19)$$

and

$$\tilde{u}(j\omega) = \Pi(j\omega)u(j\omega). \quad (2-20)$$

Then

$$\dot{z}_1 = Dz_1 + Ex, \quad (2-21)$$

$$\tilde{x} = Lz_1 + Mx, \quad (2-22)$$

and

$$\dot{z}_2 = Fz_2 + Hu, \quad (2-23)$$

$$\tilde{u} = Nz_2 + Ju. \quad (2-24)$$

The first term in (2-17) can now be rewritten using (2-18), (2-19), (2-21), and (2-22) as

$$\begin{aligned} x^*(j\omega)Q(j\omega)x(j\omega) &= x^*(j\omega)Q_1(j\omega)x(j\omega) + x^*(j\omega)\Pi^*(j\omega)Q_2^*x(j\omega) \\ &\quad + x^*(j\omega)Q_2\Pi(j\omega)x(j\omega) + x^*(j\omega)\Pi^*(j\omega)Q_3\Pi(j\omega)x(j\omega) \\ &= (x^*(j\omega) \tilde{x}^*(j\omega)) \begin{bmatrix} Q_1 & Q_2 \\ Q_2^* & Q_3 \end{bmatrix} \begin{pmatrix} x(j\omega) \\ \tilde{x}(j\omega) \end{pmatrix} \\ &= (x^*(j\omega) z_1^*(j\omega)) \begin{bmatrix} I & M^* \\ 0 & L^* \end{bmatrix} \begin{bmatrix} Q_1 & Q_2 \\ Q_2^* & Q_3 \end{bmatrix} \begin{bmatrix} I & 0 \\ M & L \end{bmatrix} \begin{pmatrix} x(j\omega) \\ z_1(j\omega) \end{pmatrix} \quad (2-25) \end{aligned}$$

Similarly, the second term becomes:

$$u^*(j\omega)R(j\omega)u(j\omega) = (z_2^*(j\omega) u^*(j\omega)) \begin{bmatrix} N^* & 0 \\ J^* & I \end{bmatrix} \begin{bmatrix} R_1 & R_2 \\ R_2^* & R_3 \end{bmatrix} \begin{bmatrix} N & J \\ 0 & I \end{bmatrix} \begin{pmatrix} z_2(j\omega) \\ u(j\omega) \end{pmatrix} \quad (2-26)$$

Finally, the whole system and the cost function can be written as:

$$\begin{aligned}
\begin{pmatrix} \dot{x} \\ \dot{z}_1 \\ \dot{z}_2 \end{pmatrix} &= \begin{bmatrix} A & 0 & 0 \\ E & D & 0 \\ 0 & 0 & F \end{bmatrix} \begin{pmatrix} x \\ z_1 \\ z_2 \end{pmatrix} + \begin{pmatrix} B \\ 0 \\ H \end{pmatrix} u \\
&= \tilde{A} \begin{pmatrix} x \\ z_1 \\ z_2 \end{pmatrix} + \tilde{B}u
\end{aligned} \tag{2-27}$$

and

$$\begin{aligned}
J &= \frac{1}{2} \int_{-\infty}^{\infty} (x^* \ z_1^* \ z_2^* \ u^*) \begin{bmatrix} \Gamma_1 & \Gamma_2 & 0 & 0 \\ \Gamma_2^* & \Gamma_3 & 0 & 0 \\ 0 & 0 & \Psi_1 & \Psi_2 \\ 0 & 0 & \Psi_2^* & \Psi_3 \end{bmatrix} \begin{pmatrix} x \\ z_1 \\ z_2 \\ u \end{pmatrix} d\omega \\
&= \frac{1}{2} \int_{-\infty}^{\infty} (x^* \ z_1^* \ z_2^* \ u^*) \begin{bmatrix} Q & S \\ S^* & R \end{bmatrix} (x \ z_1 \ z_2 \ u)^T d\omega,
\end{aligned} \tag{2-28}$$

where

$$\Gamma_1 = Q_1 + M^* Q_2^* + Q_2 M + M^* Q_3 M,$$

$$\Gamma_2 = Q_2 L + M^* Q_3 L,$$

$$\Gamma_3 = L^* Q_3 L,$$

$$\Psi_1 = N^* R_3 N,$$

$$\Psi_2 = N^* R_3 J + N^* R_2^*,$$

$$\Psi_3 = R_1 + R_2 J + J^* R_2^* + J^* R_3 J,$$

$$Q = \begin{bmatrix} \Gamma_1 & \Gamma_2 & 0 \\ \Gamma_2^* & \Gamma_3 & 0 \\ 0 & 0 & \Psi_1 \end{bmatrix},$$

$$S^* = (0 \ 0 \ \Psi_2^*),$$

$$R = \Psi_3.$$

Note this state augmentation procedure has generated a cross-state-input matrix S which has serious implications for the robustness of this control system. The gain and phase margins and gain reduction tolerance of the standard LQ system are no longer guaranteed.

D. ROBUSTNESS FOR A GENERALIZED QUADRATIC CRITERION

The addition of frequency shaping in the cost function generated a cross-state-input term. A procedure very similar to those performed on (2-9) through (2-15) is developed below to identify the effect of S on the robustness of the system. First, the following definitions are made to simplify the expression:

$$x = \begin{bmatrix} x \\ z_1 \\ z_2 \end{bmatrix}, \quad (2-29)$$

Furthermore, define

$$u' = -R^{-1}B^*Px, \quad (2-30)$$

and

$$u = u' - R^{-1}S^*x. \quad (2-31)$$

Then

$$\begin{aligned} \dot{x} &= Ax + Bu \\ &= Ax + B(u' - R^{-1}S^*x) \\ &= (A - BR^{-1}S^*)x + Bu' \\ &= A'x + Bu'. \end{aligned} \quad (2-32)$$

From (2-28),

$$\begin{aligned}
& x^* Qx + x^* Su + u^* S^* x + u^* Ru \\
&= x^* Qx + x^* S(u' - R^{-1} S^* x) + (u' - R^{-1} S^* x)^* S^* x \\
&\quad + (u' - R^{-1} S^* x)^* R(u' - R^{-1} S^* x) \\
&= x^* (Q - SR^{-1} S^*) x + u'^* Ru \\
&= x^* Q' x + u'^* Ru.
\end{aligned} \tag{2-33}$$

Using the above definitions, the SSRE becomes

$$\begin{aligned}
& PA' + A'^* P + Q' - PBR^{-1} B^* P \\
&= P(A - BR^{-1} S^*) + (A - BR^{-1} S^*)^* P + Q \\
&\quad - SR^{-1} S^* - PBR^{-1} B^* P \\
&= PA + A^* P + Q - (PB + S)R^{-1}(PB + S)^* = 0.
\end{aligned} \tag{2-34}$$

Finally,

$$\begin{aligned}
u &= u' - R^{-1} S^* x \\
&= -R^{-1} B^* P x - R^{-1} S^* x \\
&= -R^{-1} (B^* P + S^*) x,
\end{aligned} \tag{2-35}$$

and

$$K = R^{-1} (B^* P + S^*) = R^{-1} (PB + S)^* \tag{2-36}$$

Now, given the modifications as in (2-29) through (2-36) the analysis of the system proceeds just as in the standard LQ case:

$$G(s) = (sI - A)^{-1} B, \tag{2-37}$$

and

$$L(s) = KG(s) = K(sI - A)^{-1} B. \quad (2-38)$$

Using (2-36),

$$L(s) = R^{-1}(PB + S)^*(sI - A)^{-1} B. \quad (2-39)$$

Adding and subtracting sP to the SSRE and rearranging yields

$$-P(sI - A) - (sI - A^*)P + Q - (PB + S)R^{-1}(PB + S)^* = 0. \quad (2-40)$$

Multiplying from the right by $G(s)$ and from the left by $G^*(s)$ and rearranging terms as was done in (2-14) and (2-15) results in

$$[I + L(s)]^* R[I + L(s)] = R + G^*(s)QG(s) + S^*G(s) + G^*(s)S. \quad (2-41)$$

Comparing (2-41) with (2-15), there are two new terms as a result of the cross-state-input matrix S . The standard optimal LQ system was guaranteed an infinite gain margin, 50% GRT, and 60° of phase margin. If these two new terms in (2-41) result in *reducing the magnitude* of the right hand side, they will effectively reduce the robustness of the system. Of course, the converse may also be true. In some systems, the right hand side may be increased and robustness will correspondingly increase. The effects of S will depend on the particular system and the required frequency shaping in the cost function.

III. MODEL UNCERTAINTY AND ROBUSTNESS MEASURES FOR MULTIVARIABLE SYSTEMS

Multi-input multi-output (MIMO) systems introduce significantly greater complexity into the control design problem. The additional inputs and outputs provide a designer with much more flexibility in the solution to the problem of stabilizing a system, but they also complicate the subject of defining the robustness of the system. This chapter presents some concepts used for MIMO systems and develops the robustness measure to be used for this thesis.

A. MODEL UNCERTAINTY FOR MIMO SYSTEMS

Since no design model will exactly match the physical plant, it is important to consider these model uncertainties for control system design. The form used in representing them depends on the degree to which the physical mechanisms of the uncertainties are understood or known. In general, representations can be placed into two categories based on the amount of structure in the uncertainty. Highly-structured representations are those in which the amount of parameter variation can be confined within well defined limits for models at various operating points. An example would be the aerodynamic coefficients of a missile for different altitudes and velocities. Less-structured representations usually place bounds on the uncertainty of the plant transfer function. Doyle [Ref. 5] gives two general ways of representing this:

$$G'(j\omega) = G(j\omega) + \Delta G(j\omega), \quad (3-1)$$

where

$$\overline{\sigma}[\Delta G(j\omega)] < l_a(\omega) \quad \text{for } \forall \omega \geq 0 \quad (3-2)$$

and

$$G'(j\omega) = G(j\omega)[I + \Delta(j\omega)], \quad (3-3)$$

where

$$\overline{\sigma}[\Delta(j\omega)] < l_m(\omega) \quad \text{for } \forall \omega \geq 0. \quad (3-4)$$

The maximum singular value $\overline{\sigma}$ is defined by

$$\overline{\sigma}[A] \equiv \max_{\|x\|=1} \|Ax\| \equiv \sqrt{\lambda_{\max}[A^*A]} \quad (3-5)$$

Neither (3-1) and (3-2) nor (3-3) and (3-4) attempt to give any indication of the causes of the uncertainties. The additive uncertainty representation, (3-1) and (3-2), bounds the matrix G' within a region l_a about G . The multiplicative uncertainty representation, (3.3) and (3-4) (which is preferred here since it applies the same uncertainty to both uncompensated and compensated transfer functions), confines the matrix G' to a normalized neighborhood, l_m , about G . This type of uncertainty can be incorporated into the system model as shown in Figure 3.1. Knowledge about and experience with the uncertainties affecting a particular system are the determining factors in the magnitude of l_m .

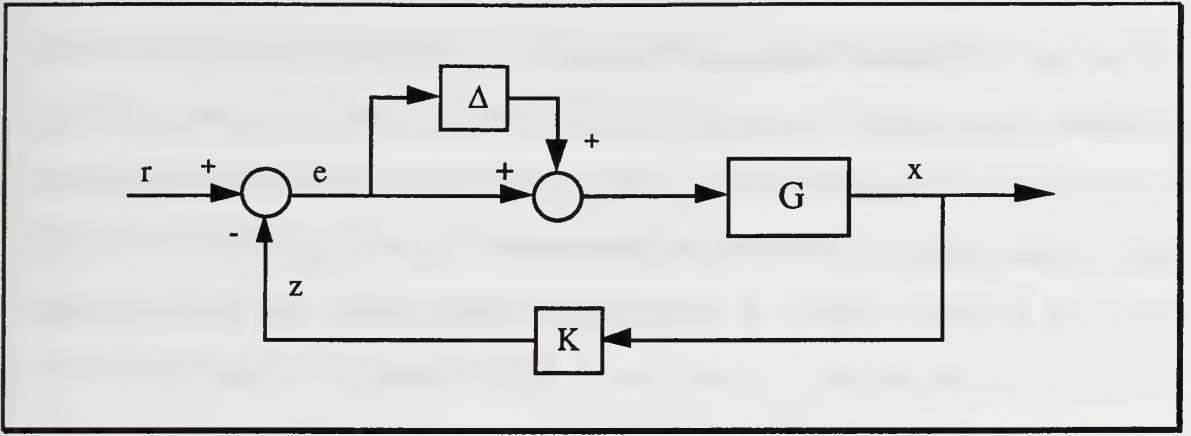


Figure 3.1 System with Unstructured Uncertainties

B. ROBUSTNESS MEASURES FOR MIMO SYSTEMS

Many methods have been investigated and developed for measuring the robustness of MIMO systems. The principal region and minimum singular value techniques will be discussed here.

1. Principal Region

Postlethwaite [Ref 6] has developed a method of extending the gain and phase margin concept to MIMO systems through the definition of a *principal region*. The principal region is found by polar decomposition of the loop transfer matrix $L(s)$:

$$L(s) = U(s)H_R(s) \quad (3-6)$$

and

$$L(s) = H_L(s)U(s), \quad (3-7)$$

where $U(s)$ is unitary and $H_R(s)$ and $H_L(s)$ are positive semi-definite Hermitian matrices with the same eigenvalues. Principal gains (or singular values) are defined as the eigenvalues of $H_R(s)$ or $H_L(s)$ and the principal phases are

defined as the phases of the eigenvalues of $U(s)$. The maximum and minimum principal gains, σ_{max} and σ_{min} , and the maximum and minimum principal phases, ϕ_{max} and ϕ_{min} , for each s , form a curvilinear rectangle in the Nyquist plane. Combining all the rectangles for values of s on the Nyquist D contour forms the principal region. A gain margin, phase margin, and gain reduction tolerance can be defined, as depicted in Figure 3.2, at the boundary of the principal region.

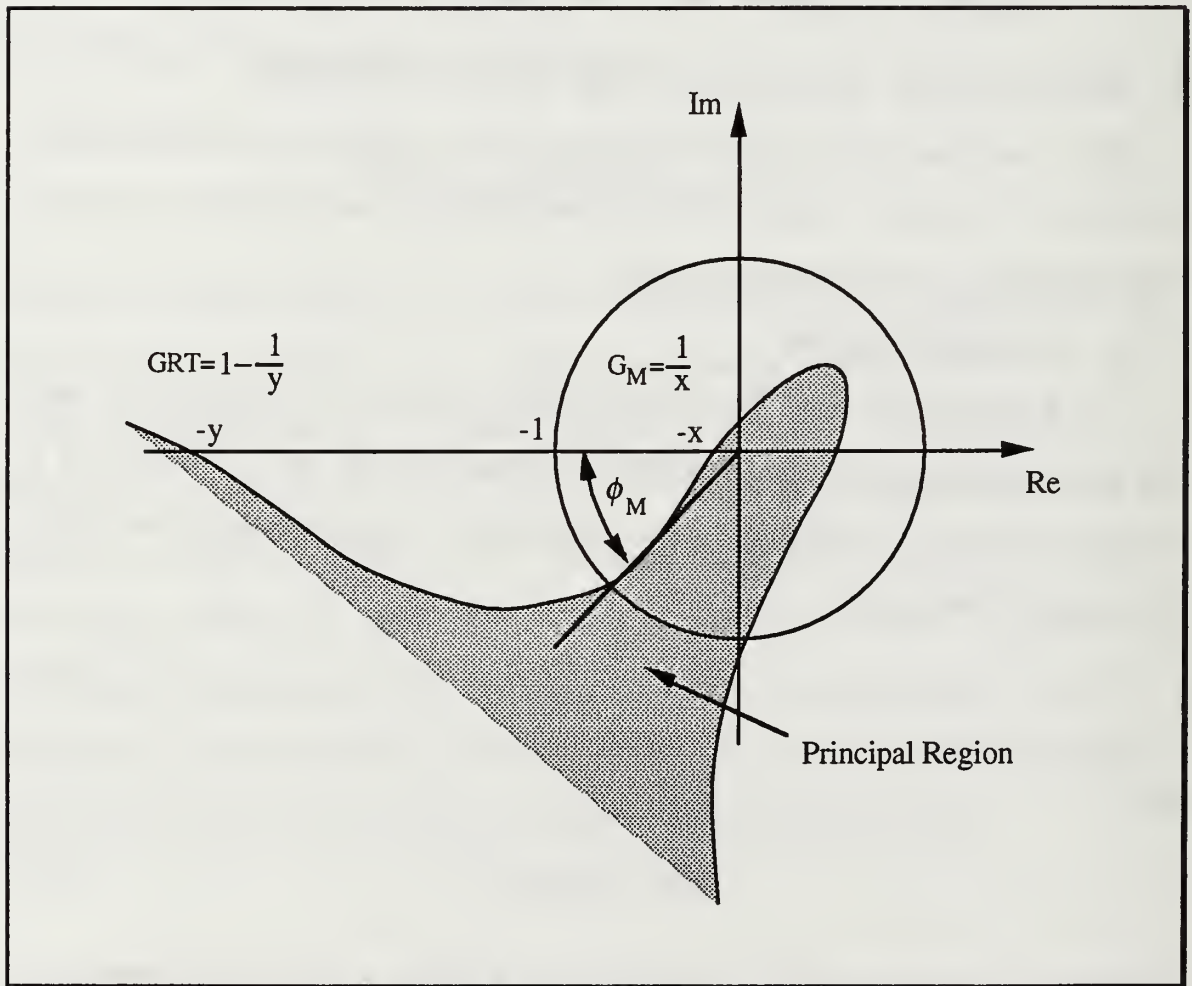


Figure 3.2 Principal Region and Stability Margins for MIMO systems [After Ref. 4]

This method generates graphical information which does not easily lead to defining a single parameter which may be used to adjust performance and robustness. However, the use of just the minimum singular values, while a more conservative approach, provides similar robustness information and does lend itself to the goal of this thesis.

2. Minimum Singular Value

A measure of the robustness of a system with the uncertainties described above can be obtained as follows:

$$z = KG(I + \Delta)e \quad (3-8)$$

and

$$e = r - z. \quad (3-9)$$

Then

$$e = r - KG(I + \Delta)e, \quad (3-10)$$

$$(I + KG(I + \Delta))e = r, \quad (3-11)$$

and

$$\begin{aligned} e &= (I + KG(I + \Delta))^{-1} r \\ &= (I + KG + KG\Delta)^{-1} r \\ &= \left[(I + KG)(I + (I + KG)^{-1} KG\Delta) \right]^{-1} r \\ &= \left[I + (I + KG)^{-1} KG\Delta \right]^{-1} (I + KG)^{-1} r. \end{aligned} \quad (3-12)$$

Using the small gain theorem and (3-12), a sufficient condition to guarantee closed-loop stability is

$$\| (I + KG)^{-1} KG \| \cdot \| \Delta \| < 1 \quad (3-13)$$

or equivalently

$$\bar{\sigma} [(I + KG)^{-1} KG] \cdot \bar{\sigma} [\Delta] < 1. \quad (3-14)$$

Using (3-4),

$$\bar{\sigma} [(I + KG)^{-1} KG] < \frac{1}{l_m} \quad (3-15)$$

Equation (3-15) can be written in a more convenient form using some results of matrix theory. First,

$$(I + KG)^{-1} KG = (I + (KG)^{-1})^{-1}, \quad (3-16)$$

so (3-15) becomes

$$\bar{\sigma} [(I + (KG)^{-1})^{-1}] < \frac{1}{l_m}. \quad (3-17)$$

and, using

$$\bar{\sigma}[A] = \frac{1}{\underline{\sigma}[A]}, \quad (3-18)$$

equation (3-17) becomes

$$\frac{1}{\underline{\sigma}[I+(KG)^{-1}]} < \frac{1}{l_m} \quad (3-19)$$

or

$$\underline{\sigma}[I+(KG)^{-1}] > l_m. \quad (3-20)$$

Therefore, the robustness measure to be used here is defined as

$$J_r \equiv \underline{\sigma}[I+(KG)^{-1}], \quad (3-21)$$

i.e., J_r is the minimum singular value for the system in the frequency range of interest. J_r is a single number which gives a measure of the robustness of the system. For the standard optimal LQ system, J_r is guaranteed to be ≥ 0.5 . Therefore, the robustness of a system can be computed and directly compared to the standard optimal system and a determination made as whether or not it is satisfactory.

As stated before, this method is very conservative. There are the same number of singular values as the dimension of the system and it is unlikely that the uncertainties in the model will affect the whole system equally across all the states. Therefore, some models may very well have much more robustness than what is predicted by this method.

IV. ROBUST SUBOPTIMAL DESIGN

The general idea for the suboptimal robust design is to trade off optimality (i.e., performance) for a greater degree of robustness. In the case of the generalized linear quadratic control system, this means computing the feedback gains, $K = R^{-1}(PB + S)^*$, by modifying Q , R , or S in (2-41).

A number of design possibilities exist and seven options investigated under this thesis work are presented below.

A. ROBUSTNESS DESIGN OPTIONS

Equation (2-41) is repeated here as it serves as the basis for evaluating robustness:

$$(I + L)^* R(I + L) = R + G^* Q G + S^* G + G^* S, \quad (4-1)$$

where L and G are understood to be functions of $s = j\omega$. In addition, using the relation

$$(R + S^* G)^* R^{-1} (R + S^* G) = R + S^* G + G^* S + G^* S R^{-1} S^* G, \quad (4-2)$$

equation (4-1) can be rewritten as

$$(I + L)^* R(I + L) = G^* (Q - S R^{-1} S^*) G + (R + S^* G)^* R^{-1} (R + S^* G). \quad (4-3)$$

Note that the right side is guaranteed to be greater than or equal to zero if

$$Q - S R^{-1} S^* \geq 0. \quad (4-4)$$

The greater the right side of (4-3) the better the robustness and it certainly needs to be greater than zero to guarantee stability. All options are presented using a tilde, \sim , to indicate the modified parameters.

1. Option I: $\tilde{S} = 0$

The first option is to simply ignore the cross-state-input matrix by setting $\tilde{S} = S = 0$. Equation (4-1) would be reduced to

$$(I + L)^* R(I + L) = R + G^* QG, \quad (4-5)$$

which is the same as (2-15) for the standard LQ situation. However, this is just a special case of option IV.

2. Option II: $\tilde{Q} = Q + SS^*$, $\tilde{R} = R + I$

These substitutions yield

$$(I + L)^* \tilde{R}(I + L) = \tilde{R} + G^* \tilde{Q}G + S^* G + G^* S \quad (4-6)$$

or

$$(I + L)^* (R + I)(I + L) = R + G^* QG + (I + S^* G)^* (I + S^* G). \quad (4-7)$$

Here the terms on the right hand side have either been forced into quadratic forms or are positive, ensuring that robustness is improved.

3. Option III: $\tilde{R} = \rho R$

This is a straight-forward introduction of a multiplicative parameter into (4-1) which gives

$$\begin{aligned} (I + L)^* \tilde{R}(I + L) &= \tilde{R} + G^* QG + S^* G + G^* S \\ &= \rho R + G^* QG + S^* G + G^* S \end{aligned} \quad (4-8)$$

or

$$(I+L)^* R(I+L) = R + \frac{1}{\rho} (G^* QG + S^* G + G^* S). \quad (4-9)$$

As ρ is increased, the right side approaches R . If the robustness of the system had originally been degraded by S , theoretically, the best that could be achieved by this option is exactly the minimum guaranteed by the standard LQ system.

4. Option IV: $\tilde{S} = \rho S$, $\rho \leq 1$

As in option III, this is also a simple substitution using a multiplicative parameter. This time, however, it is applied directly to S :

$$\begin{aligned} (I+L)^* R(I+L) &= R + G^* QG + \tilde{S}^* G + G^* \tilde{S} \\ &= R + G^* QG + \rho(S^* G + G^* S) \end{aligned} \quad (4-10)$$

Note that when $\rho = 0$, (4-9) reduces to

$$(I+L)^* R(I+L) = R + G^* QG, \quad (4-11)$$

the standard optimal LQ case and option I is therefore, a special subset of this option.

5. Option V: $\tilde{R} = \rho R$, $\tilde{Q} = Q + (\rho - 1)SR^{-1}S^*$, $\rho \geq 1$

Substituting into (4-3):

$$(I+L)^* \tilde{R}(I+L) = G^* [\tilde{Q} - SR^{-1}S^*]G + (\tilde{R} + S^* G)^* \tilde{R}^{-1}(\tilde{R} + S^* G). \quad (4-12)$$

This results in

$$(I+L)^* \rho R(I+L) = G^* [Q + (\rho - 2)SR^{-1}S^*]G \\ + (\rho R + S^*G)^* (\rho R)^{-1} (\rho R + S^*G) \quad (4-13)$$

or

$$(I+L)^* R(I+L) = \frac{1}{\rho} G^* [Q + (\rho - 2)SR^{-1}S^*]G \\ + (R + \frac{1}{\rho} S^*G)^* R^{-1} (R + \frac{1}{\rho} S^*G). \quad (4-14)$$

As ρ is increased, (4-14) approaches

$$(I+L)^* R(I+L) = R + G^* SR^{-1}S^*G. \quad (4-15)$$

Again, the term with S has been made quadratic in order to improve robustness.

6. Option VI: $\tilde{Q} = \rho Q$

Here, a simple substitution of a multiplicative parameter into (4-3):

$$(I+L)^* R(I+L) = G^* [\tilde{Q} - SR^{-1}S^*]G \\ + (R + S^*G)^* R^{-1} (R + S^*G) \quad (4-16)$$

or

$$(I+L)^* R(I+L) = G^* [\rho Q - SR^{-1}S^*]G \\ + (R + S^*G)^* R^{-1} (R + S^*G). \quad (4-17)$$

Note that the right side is guaranteed to be greater than or equal to zero only if

$$\rho Q - SR^{-1}S^* \geq 0. \quad (4-18)$$

For optimal LQ theory, Q is only required to be positive *semi-definite*. For this option, there is no guarantee that $\rho Q - SR^{-1}S^*$ can be made greater than zero unless Q is positive *definite*.

7. Option VII: $\tilde{Q} = Q + \rho SR^{-1}S^*$, $\rho \geq 1$

Substituting \tilde{Q} into (4-3) yields:

$$\begin{aligned}
 (I+L)^* R(I+L) &= G^* [\tilde{Q} - SR^{-1}S^*] G \\
 &\quad + (R+S^*G)^* R^{-1} (R+S^*G) \\
 &= G^* [Q + (\rho - 1)SR^{-1}S^*] G \\
 &\quad + (R+S^*G)^* R^{-1} (R+S^*G) \quad (4-19)
 \end{aligned}$$

Again, the right side is greater than or equal to zero for $\rho \geq 1$.

This list certainly does not exhaust the possibilities, but it does provide many avenues for investigation of the robustness of an MIMO system optimized by a general quadratic criterion. It should also be noted that when Q , R , or S is modified, the control system is no longer optimal.

V. A NUMERICAL EXAMPLE AND SIMULATION

To explore the utility of the theory so far developed, a numerical example will be presented and the control systems using the various options in the preceding chapter will be designed and simulated. The model to be used is the one used by Chen [Ref. 3]. The development and explanation of this model is briefly summarized here. The simulations will use a wind gust as the disturbance input to the system to test the transient response of various suboptimal designs.

A. STATICALLY UNSTABLE AIRCRAFT MODEL

The model for this simulation is the F-20 Tigershark designed by Northrop Corp. The aircraft is designed to be extremely agile, and as a result, is highly unstable in the absence of a control system. In addition, the simulation will be based on a special flight mode called *fuselage-pitch-pointing* (FPP) mode. The fuselage-pitch-pointing concept provides the ability to alter the pitch without changing the flight path (Figure 5.1). Another interesting flight mode called *direct lifting* (DL) is shown in Figure 5.2, where the aircraft's altitude can be changed without changing the pitch.

These are not the intuitive ways of flying an aircraft and therefore, would not be the normal modes of operation. Instead, it might be used in special circumstances such as bombing runs or during dogfights where the ability to rapidly change altitude or pitch of the aircraft independently may provide significant advantage over an adversary. In addition, the FPP mode provides a good MIMO model for investigating robust, suboptimal controller design.

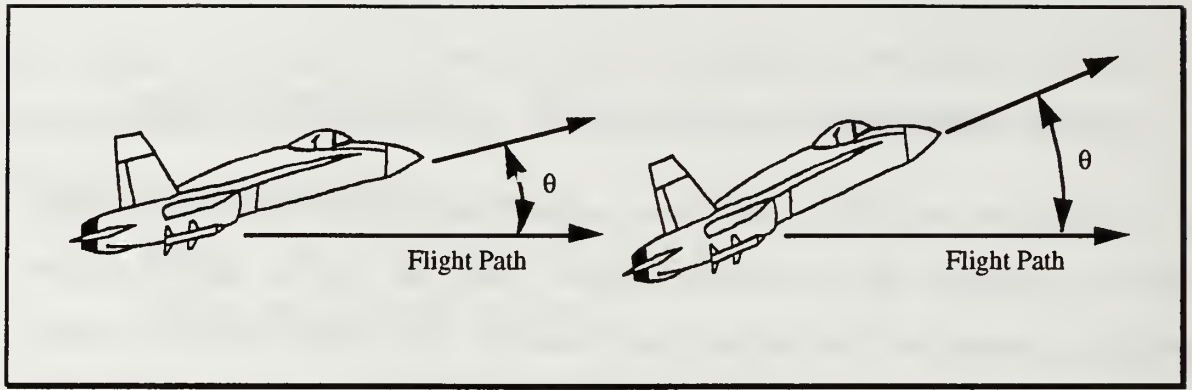


Figure 5.1 Pitch Pointing, Constant Flight Path

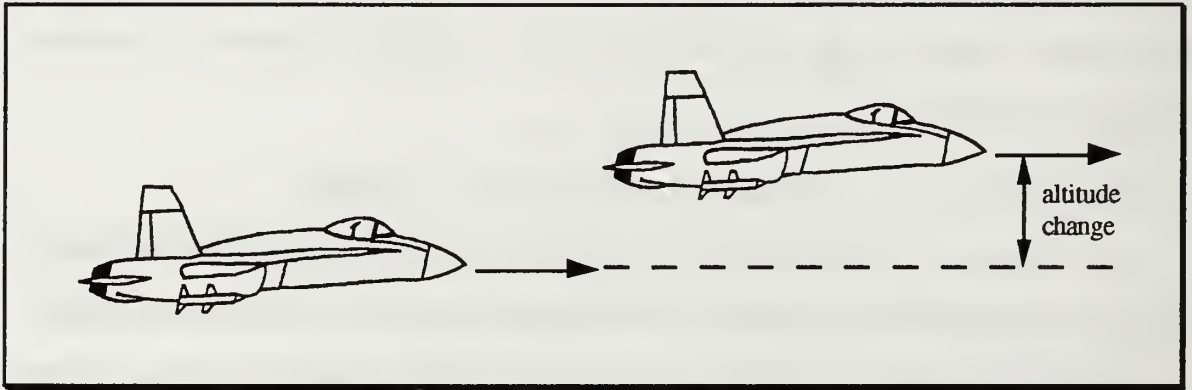


Figure 5.2 Direct Lifting, Constant Pitch

A linearized pitch-axis model for the F-20 at Mach 0.5 and an altitude of 10,000 feet is:

$$\begin{bmatrix} \dot{\alpha} \\ \dot{q} \\ \dot{\theta} \end{bmatrix} = \begin{bmatrix} -0.834 & 0.996 & 0 \\ 2.755 & -0.89 & 0 \\ 0 & 1.0 & 0 \end{bmatrix} \begin{bmatrix} \alpha \\ q \\ \theta \end{bmatrix} + \begin{bmatrix} -0.2 & -0.093 \\ -11.4 & 2.03 \\ 0 & 0 \end{bmatrix} \begin{bmatrix} \delta_h \\ \delta_f \end{bmatrix} \quad (5-1)$$

$$y = \begin{bmatrix} \alpha \\ q \\ \theta \end{bmatrix} \quad (5-2)$$

The state variables are angle of attack α , pitch rate q and pitch angle θ , as shown in Figure 5.3.

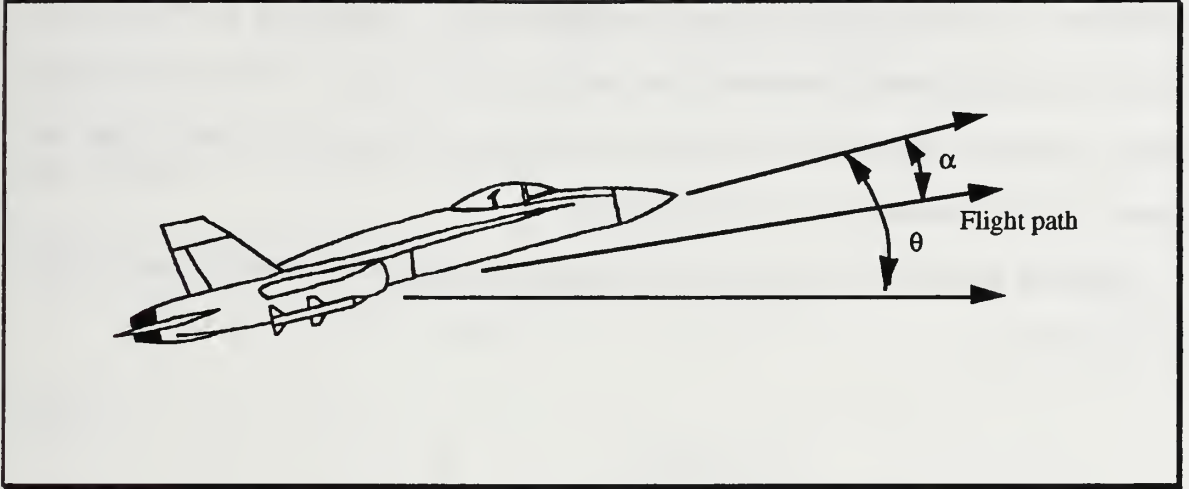


Figure 5.3 Definitions of State Variables α , q , and θ

The two control inputs are stabilizer position δ_h and trailing edge flap position δ_f . This model has three poles located at $s = 0, -2.519$, and 0.795 .

The design problem is to develop an FPP control system that will reject turbulence and yet provide good robustness. This thesis will focus on a regulator type of control which will endeavor to maintain the states of the system at desired values in the presence of disturbances to the system. An appropriate frequency-shaped quadratic cost function which accomplishes these objectives is

$$J_c = \int_{-\infty}^{\infty} [150\alpha^2 + q^2 + 50(\theta - \alpha) + \left(\frac{j\omega}{j\omega + 30} \right)^2 (\delta_h^2 + 0.04\delta_f^2)] d\omega. \quad (5-3)$$

Turbulence is typically manifested by disturbance at frequencies ≤ 30 rad/sec. Therefore, the cost function is designed with a high pass filter on the control

inputs to allow greater control effort at low frequencies and to penalize control effort at higher frequencies. In addition, flight path angle $\gamma = \theta - \alpha$ is heavily weighted to limit deviations from the flight path. Turbulance however, is a transient phenomenon, therefore this optimization focuses more on rejecting these transitory disturbances in pitch rate, pitch, and angle of attack than on steady-state deviations from the flight path.

For this problem, the frequency dependent weighting matrix on the control is selected to be

$$R(j\omega) = \begin{bmatrix} \left(\frac{j\omega}{j\omega + 30} \right)^2 & 0 \\ 0 & (0.04) \left(\frac{j\omega}{j\omega + 30} \right)^2 \end{bmatrix} \quad (5-4)$$

and it can be readily decomposed into

$$\begin{aligned} & \begin{bmatrix} 0 & 0 \\ 0 & 0 \end{bmatrix} + \begin{bmatrix} \frac{j\omega}{j\omega + 30} & 0 \\ 0 & \frac{j\omega}{j\omega + 30} \end{bmatrix} \begin{bmatrix} 0 & 0 \\ 0 & 0 \end{bmatrix} + \begin{bmatrix} 0 & 0 \\ 0 & 0 \end{bmatrix} \begin{bmatrix} \frac{j\omega}{j\omega + 30} & 0 \\ 0 & \frac{j\omega}{j\omega + 30} \end{bmatrix} \\ & + \begin{bmatrix} \frac{j\omega}{j\omega + 30} & 0 \\ 0 & \frac{j\omega}{j\omega + 30} \end{bmatrix} \begin{bmatrix} 1.0 & 0 \\ 0 & 0.04 \end{bmatrix} \begin{bmatrix} \frac{j\omega}{j\omega + 30} & 0 \\ 0 & \frac{j\omega}{j\omega + 30} \end{bmatrix}, \quad (5-5) \end{aligned}$$

which meets the criteria of (2-22).

Following the augmentation procedure described in Chapter II, this system can be expressed in a frequency-independent format. First, expand the input terms of (5-3) into the form:

$$\begin{bmatrix} \frac{s}{s+30} \delta_h & \frac{s}{s+30} \delta_f \end{bmatrix} \begin{bmatrix} 1.0 & 0 \\ 0 & 0.04 \end{bmatrix} \begin{bmatrix} \frac{s}{s+30} \delta_h \\ \frac{s}{s+30} \delta_f \end{bmatrix}. \quad (5-6)$$

Now define

$$u_1 = \frac{s}{s+30} \delta_h = \left(1 - \frac{30}{s+30} \right) \delta_h, \quad (5-7)$$

and let

$$z_1 = \frac{30}{s+30} \delta_h. \quad (5-8)$$

This results in the new state equations:

$$\dot{z}_1 = -30z_1 + 30\delta_h \quad (5-9)$$

and

$$u_1 = -z_1 + \delta_h. \quad (5-10)$$

Similar steps for δ_h result in:

$$\dot{z}_2 = -30z_2 + 30\delta_f \quad (5-11)$$

and

$$u_2 = -z_2 + \delta_f. \quad (5-12)$$

Thus the new augmented system is

$$\begin{bmatrix} \dot{\alpha} \\ \dot{q} \\ \dot{\theta} \\ \dot{z}_1 \\ \dot{z}_2 \end{bmatrix} = \begin{bmatrix} -0.834 & 0.996 & 0 & 0 & 0 \\ 2.755 & -0.89 & 0 & 0 & 0 \\ 0 & 1.0 & 0 & 0 & 0 \\ 0 & 0 & 0 & -30.0 & 0 \\ 0 & 0 & 0 & 0 & -30.0 \end{bmatrix} \begin{bmatrix} \alpha \\ q \\ \theta \\ z_1 \\ z_2 \end{bmatrix}$$

$$+ \begin{bmatrix} -0.2 & -0.093 \\ -11.4 & 2.03 \\ 0 & 0 \\ 30.0 & 0 \\ 0 & 30.0 \end{bmatrix} \begin{bmatrix} \delta_h \\ \delta_f \end{bmatrix} \quad (5-13)$$

and the frequency-independent cost function is

$$J_c = \int_0^\infty [\alpha \quad q \quad \theta \quad z_1 \quad z_2 \quad \delta_h \quad \delta_f]$$

$$\cdot \begin{bmatrix} 200 & 0 & -50 & 0 & 0 & 0 & 0 \\ 0 & 1 & 0 & 0 & 0 & 0 & 0 \\ -50 & 0 & 50 & 0 & 0 & 0 & 0 \\ 0 & 0 & 0 & 1 & 0 & -1 & 0 \\ 0 & 0 & 0 & 0 & 0.04 & 0 & -0.04 \\ 0 & 0 & 0 & -1 & 0 & 1 & 0 \\ 0 & 0 & 0 & 0 & -0.04 & 0 & 0.04 \end{bmatrix} \begin{bmatrix} \alpha \\ q \\ \theta \\ z_1 \\ z_2 \\ \delta_h \\ \delta_f \end{bmatrix} dt. \quad (5-14)$$

B. SIMULATIONS

The simulations will use a vertical wind gust with a maximum velocity of 62.5 feet per second. This disturbance δ will be introduced into the system as shown in Figure 5.4. The wind gust effectively changes the direction of the incident wind and consequently the angle of attack of the aircraft, as indicated in Figure 5.5.

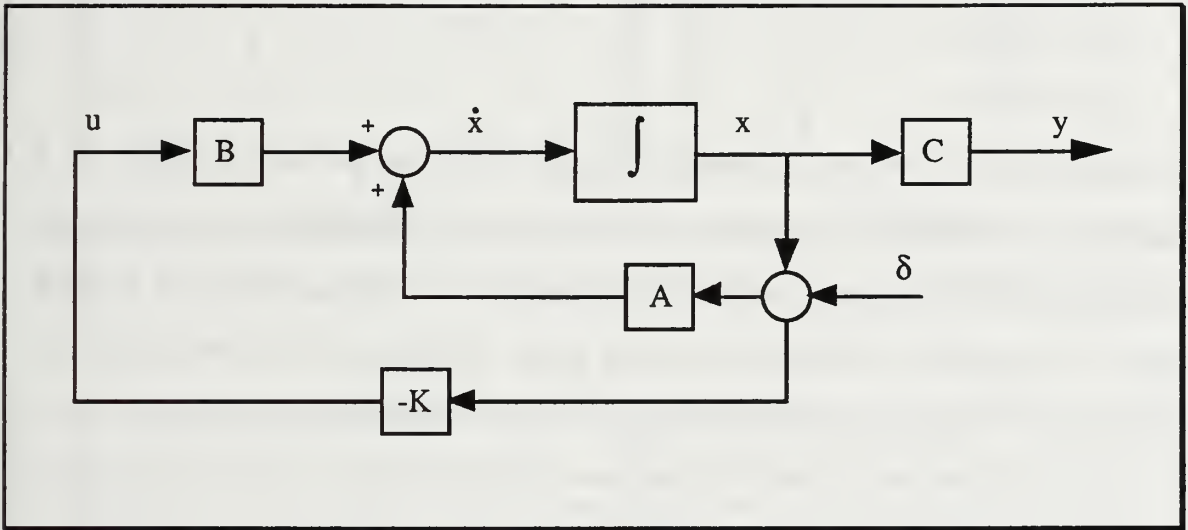


Figure 5.4 Wind Gust Disturbance Inputs

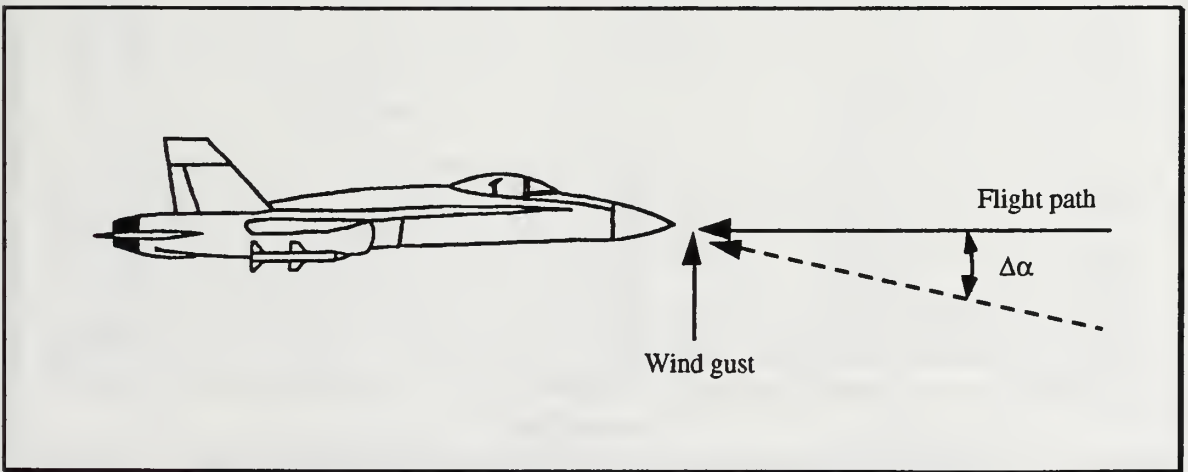


Figure 5.5 Angle of Attack

All performance J_c and robustness J_r values for these simulations are computed using the rectangular wind gust. For comparison purposes, the optimal system response is presented first.

1. Optimal System

Optimization of this control problem results in

$$K = \begin{bmatrix} -11.1747 & -1.2199 & -0.5267 & -0.3593 & -0.0169 \\ -37.0471 & 3.1484 & 35.2571 & -0.6706 & -0.5002 \end{bmatrix},$$

$$J_c = 3.9678,$$

$$J_r = 0.3529,$$

and Figure 5.6 shows the minimum singular values, as defined in (3-21), as a function of frequency. Note that within the range of frequencies expected for turbulence (≤ 30 rad/sec), the plot drops below 0.5. Figures 5.7 and 5.8 show that the response to turbulence is quite good. However, with a robustness of 0.3529, GRT is only 35 percent, leaving a much reduced margin for errors or

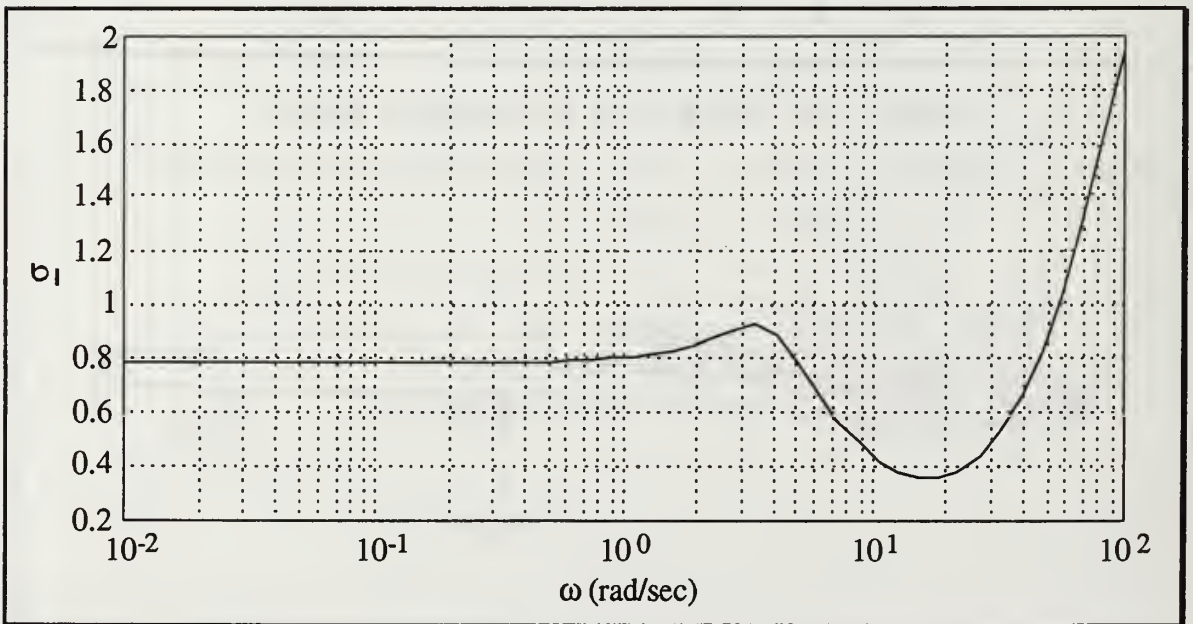


Figure 5.6 Minimum Singular Values of the Optimal System

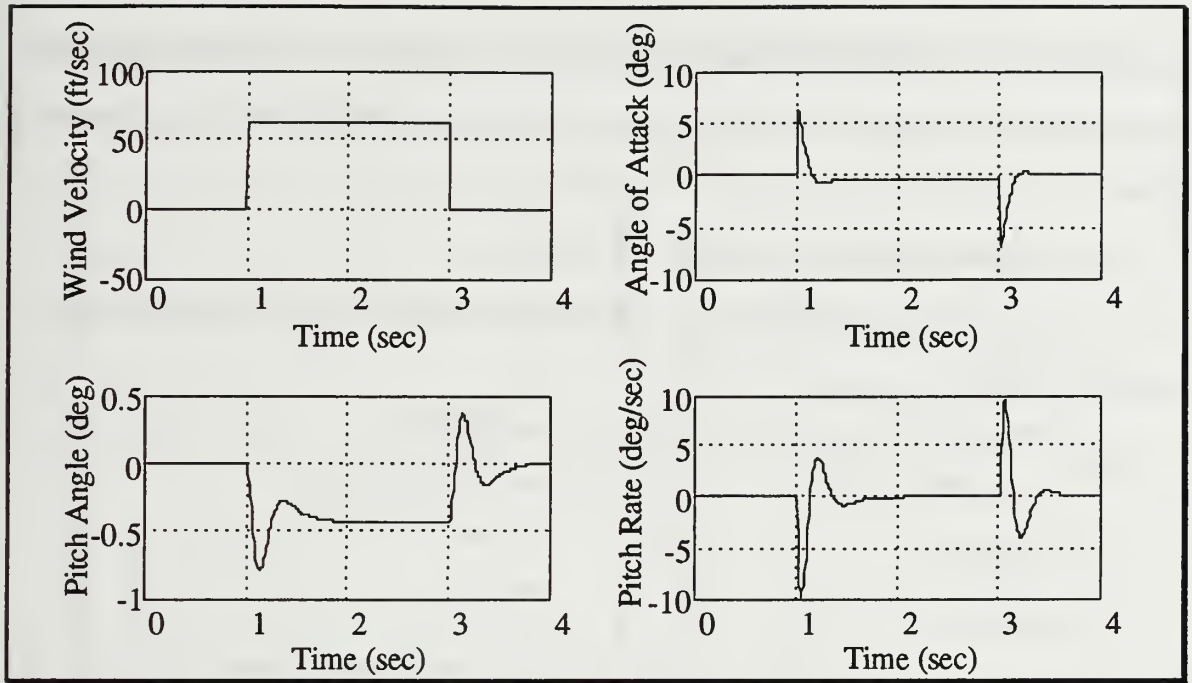


Figure 5.7 Response of the Optimal System to a Rectangular Gust

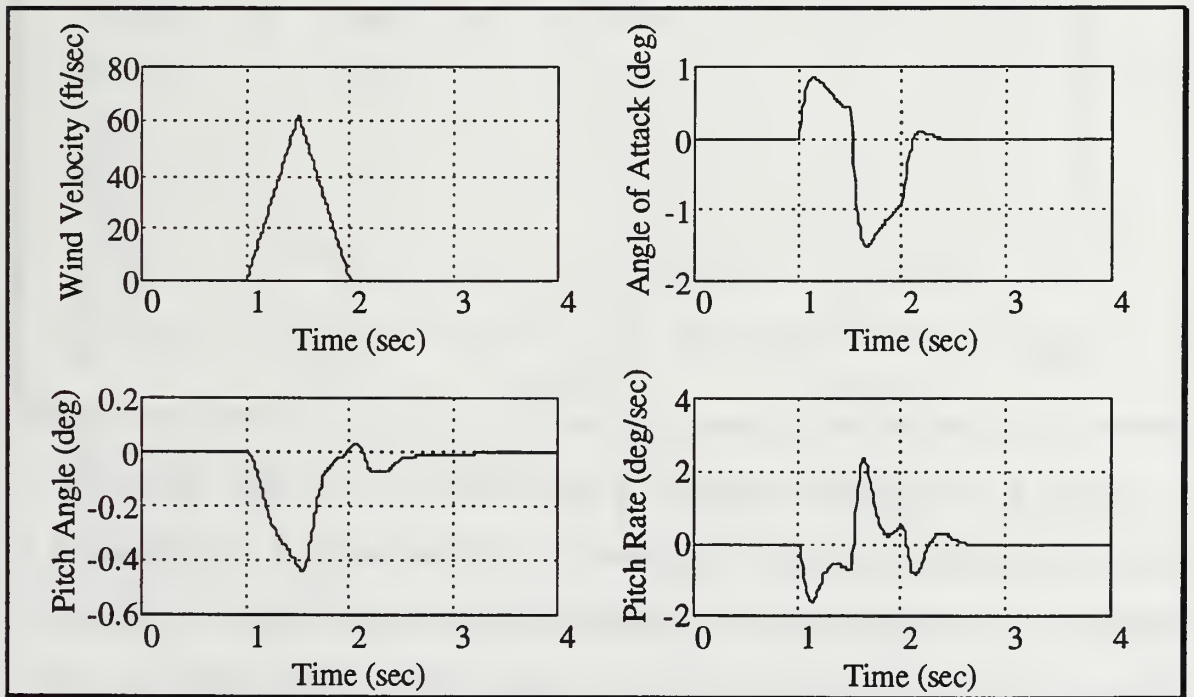


Figure 5.8 Response of the Optimal System to a Triangular Gust

uncertainties. A suboptimal design will be able to trade off some of the desired performance in order to recover greater tolerance of model and parameter error.

2. System with $\tilde{Q} = Q + SS^*$, $\tilde{R} = R + I$

This simple modification to Q and R results in the singular values shown in Figure 5.9, with

$$K = \begin{bmatrix} -6.2110 & -1.2014 & -1.9775 & 0 & -0.0008 \\ -5.1028 & 0.4075 & 6.3684 & 0 & -0.0179 \end{bmatrix},$$

$$J_c = 11.1382,$$

$$J_r = 0.8049.$$

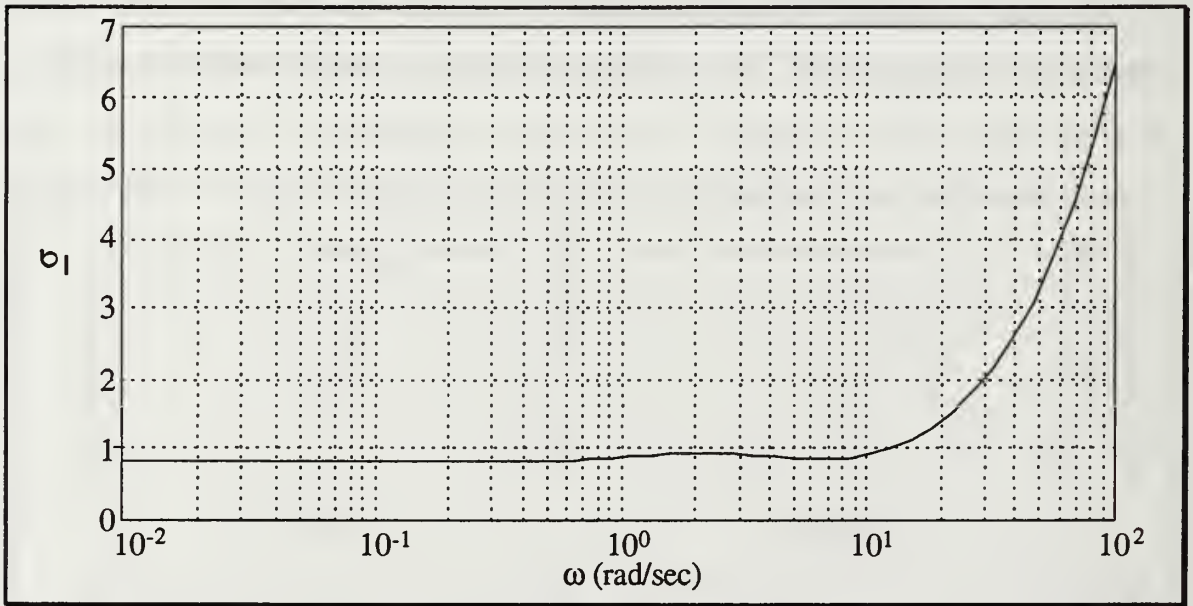


Figure 5.9 Minimum Singular Values Using $\tilde{Q} = Q + SS^*$, $\tilde{R} = R + I$

This is a significant increase in robustness. Unfortunately, it also produces a significant loss of performance, as depicted in Figures 5.10 and 5.11. There is nearly an order of magnitude increase in pitch angle, at least twice as much pitch rate, and a significant drop in response time. Additionally, there is no

adjustable parameter available for selecting some intermediate point between this and the optimal system.

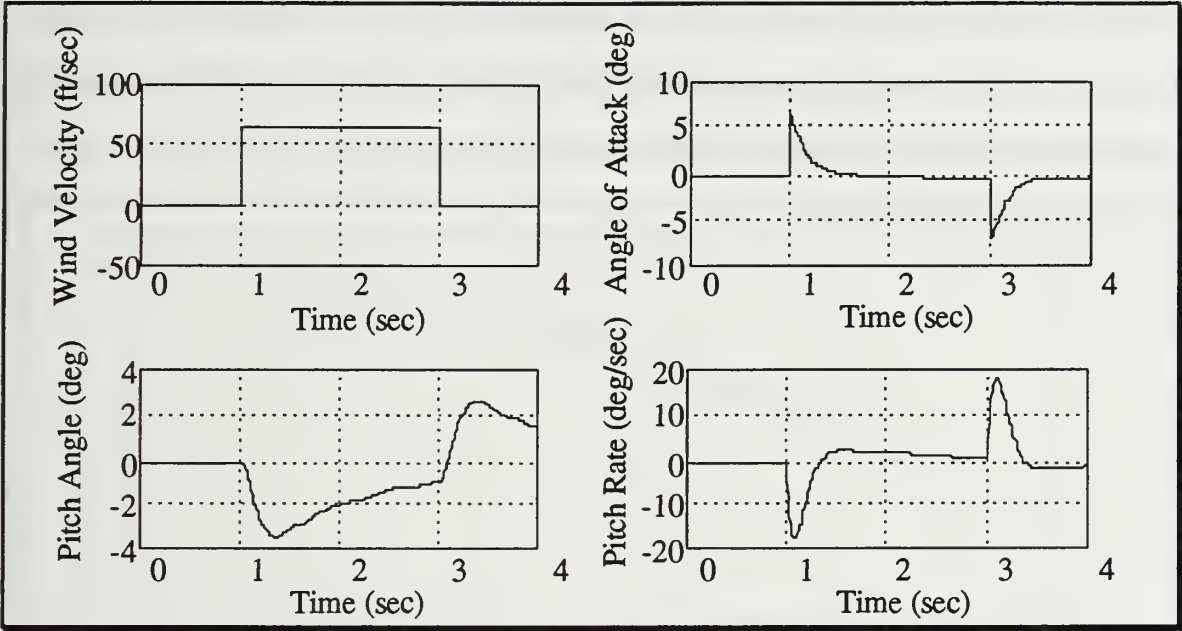


Figure 5.10 Square Gust Response of $\tilde{Q} = Q + SS^*$, $\tilde{R} = R + I$

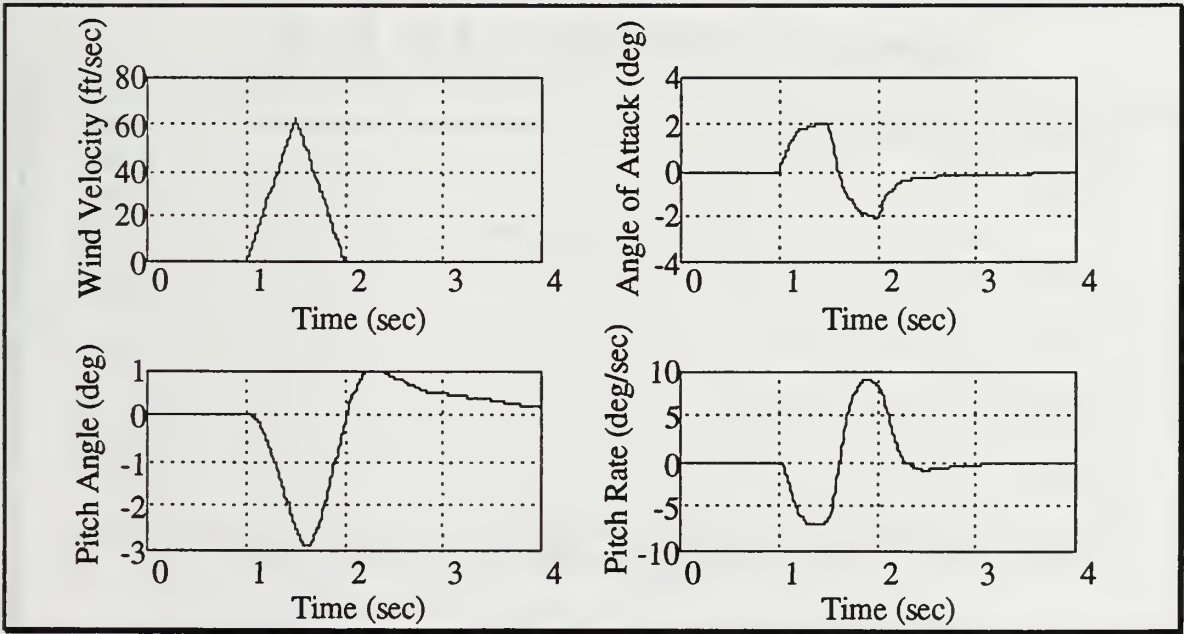


Figure 5.11 Triangular Gust Response of $\tilde{Q} = Q + SS^*$, $\tilde{R} = R + I$

3. System with $\tilde{R} = \rho R$

This option provides for adjustment of the amount of trade off. As can be seen in Figures 5.12 and 5.13, some improvement in robustness is obtained, but the maximum for this system is only 0.4583 for $\rho = 3.4$. This option appears to provide very limited and insufficient improvement.

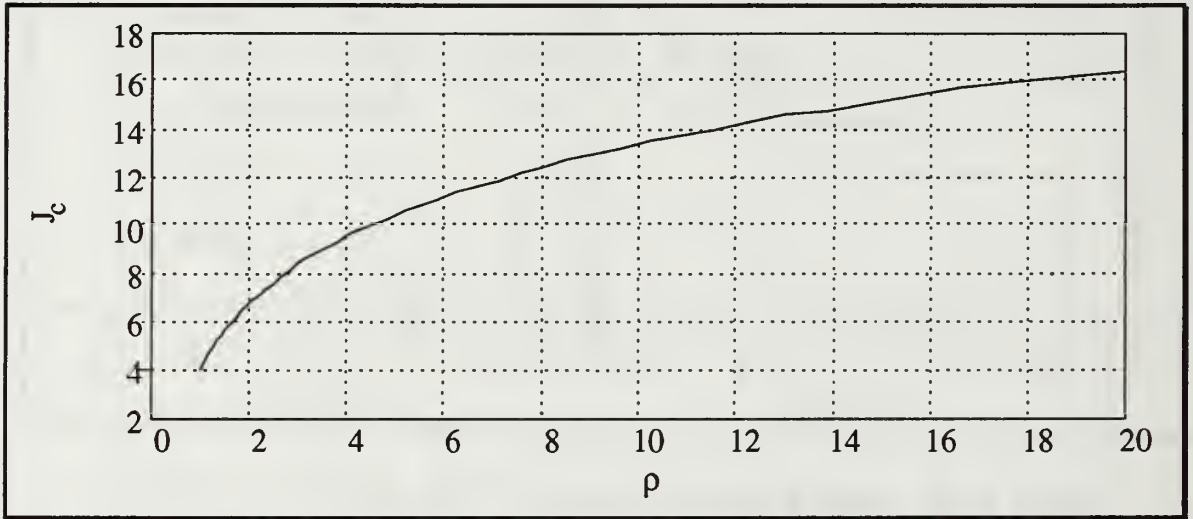


Figure 5.12 Performance vs ρ for $\tilde{R} = \rho R$

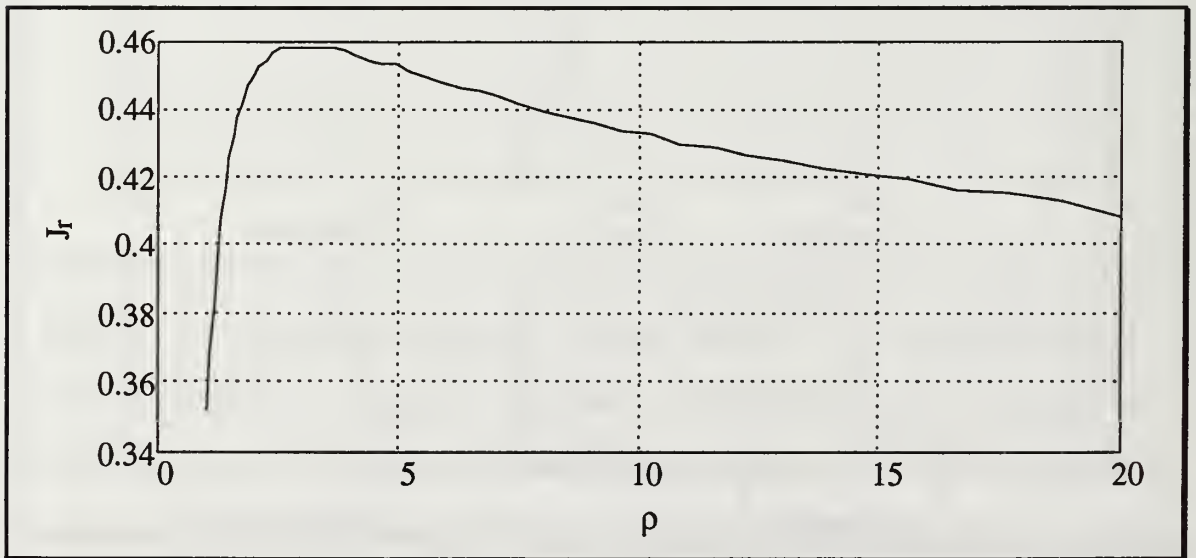


Figure 5.13 Robustness vs ρ for $\tilde{R} = \rho R$

4. System with $\tilde{S} = \rho S$, $\rho \leq 1$

This option appears to hold great promise. Comparing Figures 5.14 and 5.15 with 5.12 and 5.13, this scheme provides significantly greater increase in robustness for a much smaller loss of performance. Moreover, the use of a simple multiplicative parameter ρ allows control engineers to adjust the amount

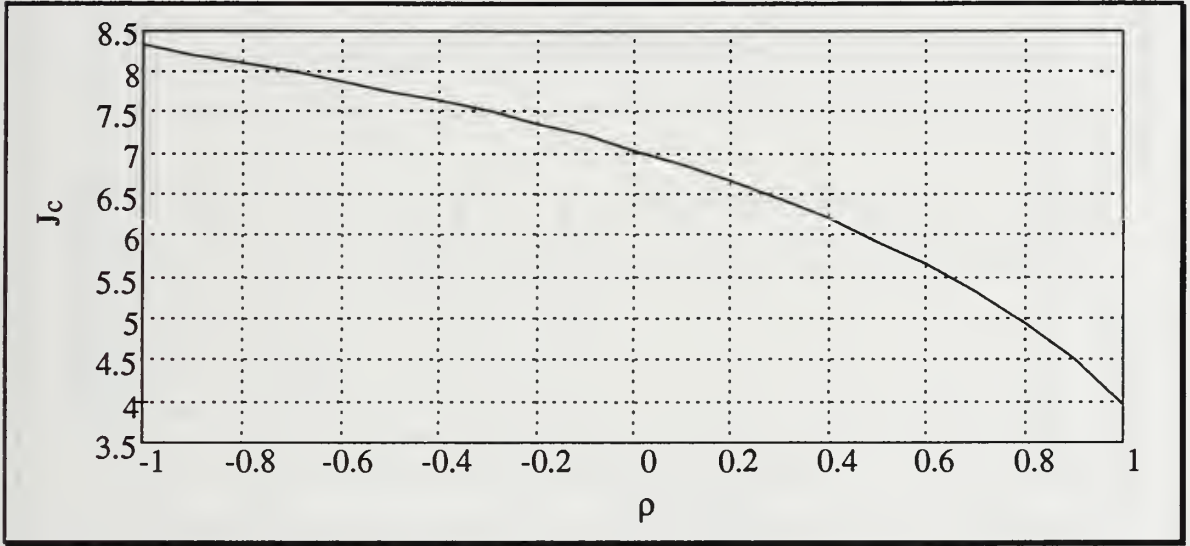


Figure 5.14 Performance vs ρ for $\tilde{S} = \rho S$, $\rho \leq 1$

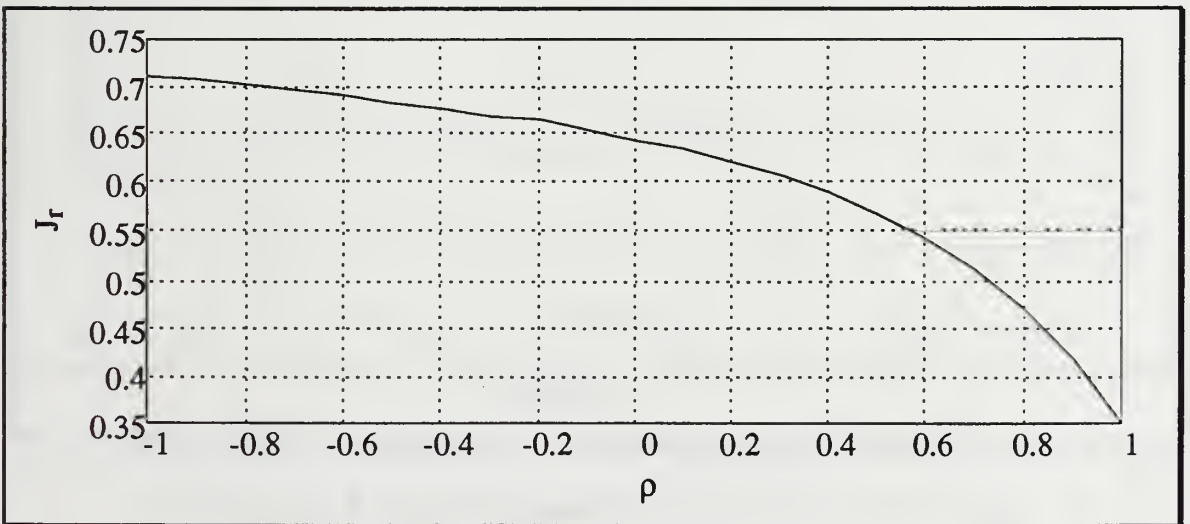


Figure 5.15 Robustness vs ρ for $\tilde{S} = \rho S$, $\rho \leq 1$

engineers to adjust the amount of trade-off. Figures 5.16 and 5.17 demonstrate the response to the two disturbances.

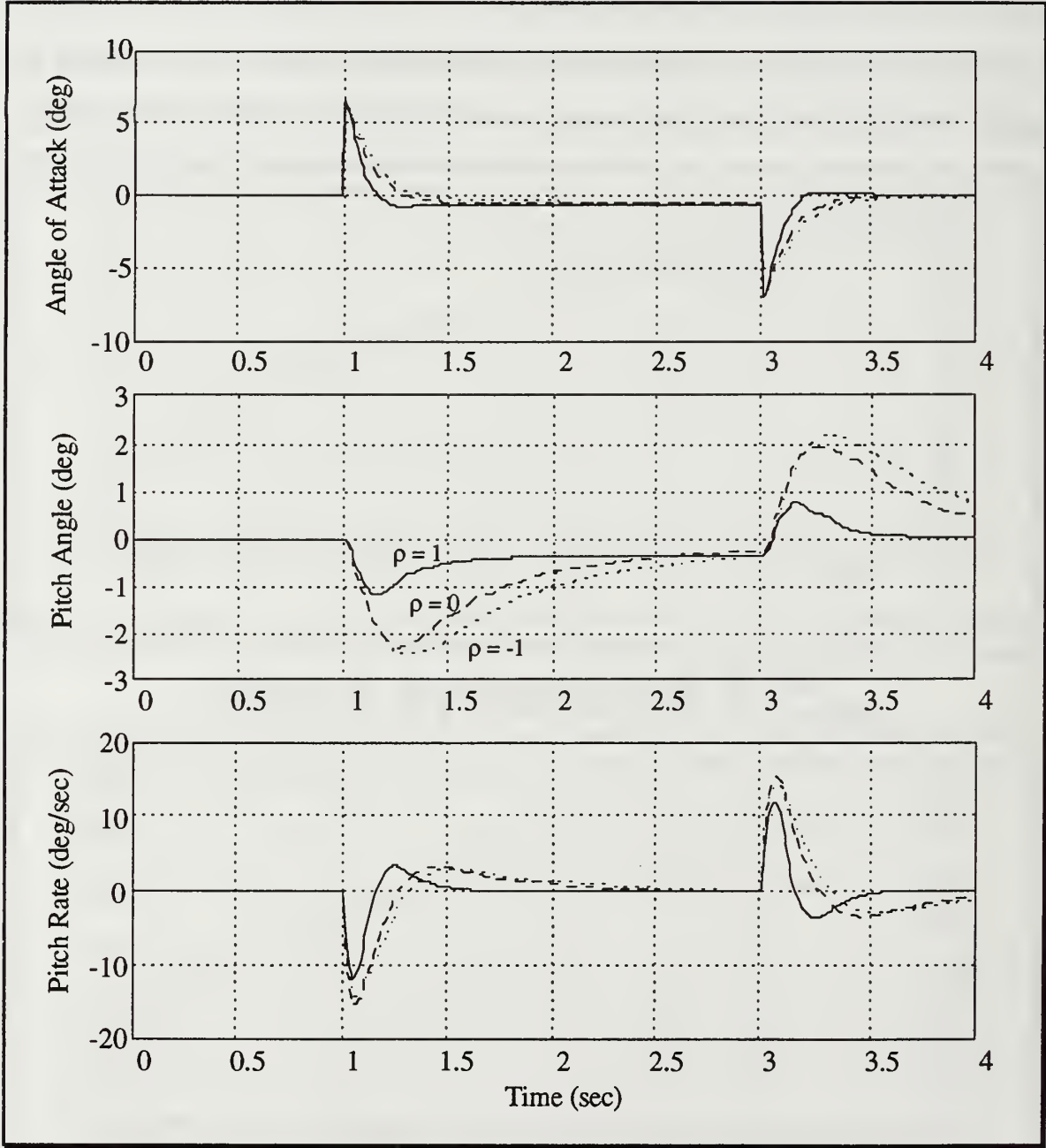


Figure 5.16 Square Gust Response for $\tilde{S} = \rho S$, $\rho \leq 1$

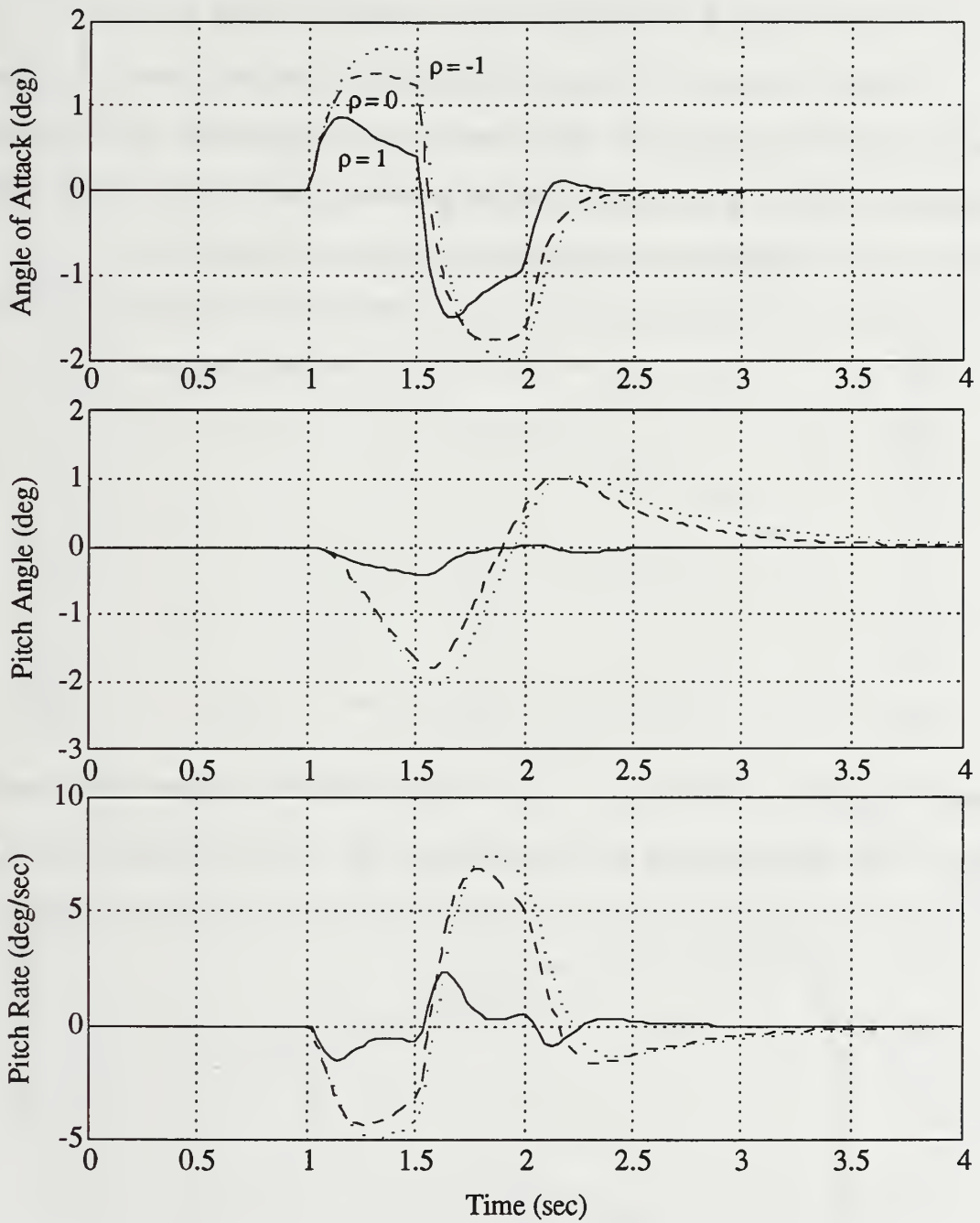


Figure 5.17 Triangular Gust Response for $\tilde{S} = \rho S$, $\rho \leq 1$

5. System with $\tilde{R} = \rho R$, $\tilde{Q} = Q + (\rho - 1)SR^{-1}S^*$, $\rho \geq 1$

Figures 5.18 and 5.19 show that although J_r does get above 0.5, there is still limited improvement for the increased cost. Apparently applying the modifications directly to the control weighting matrix provides little benefit. The responses to the disturbances are presented in Figures 5.20 and 5.21.

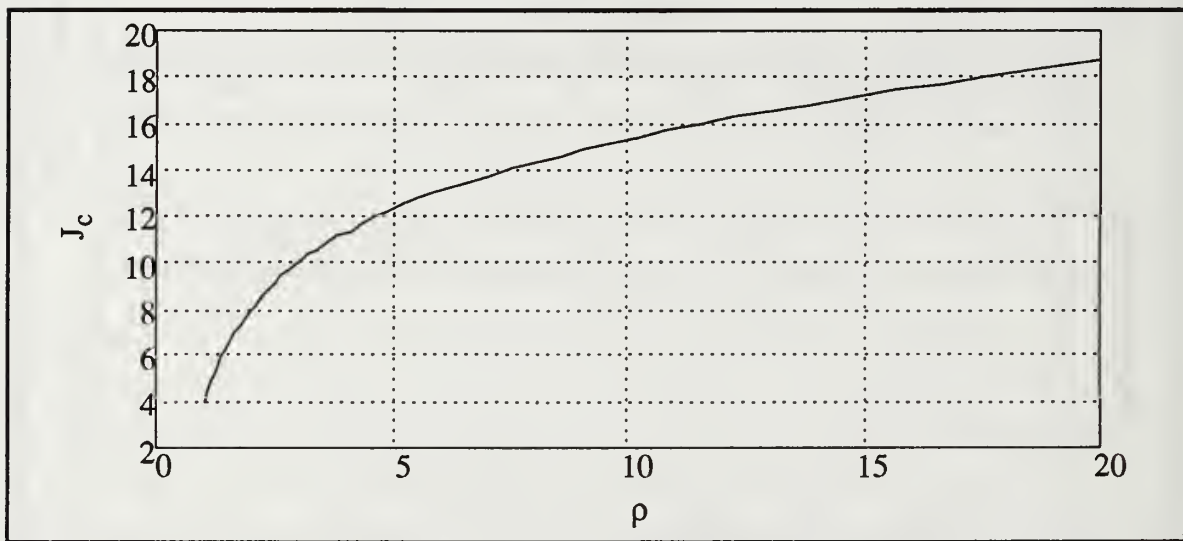


Figure 5.18 Performance vs ρ for $\tilde{R} = \rho R$, $\tilde{Q} = Q + (\rho - 1)SR^{-1}S^*$, $\rho \geq 1$

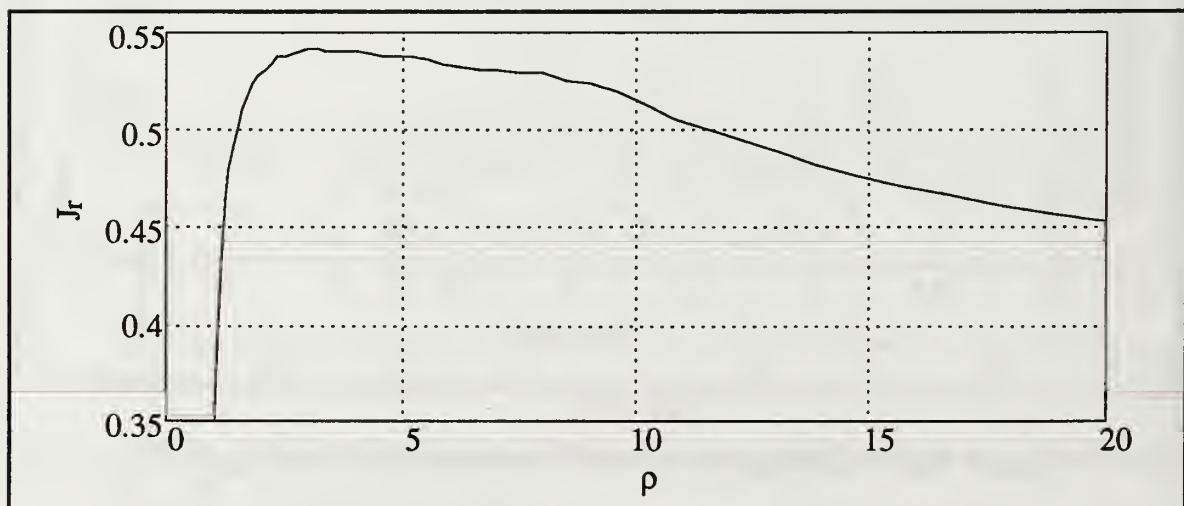


Figure 5.19 Robustness vs ρ for $\tilde{R} = \rho R$, $\tilde{Q} = Q + (\rho - 1)SR^{-1}S^*$, $\rho \geq 1$

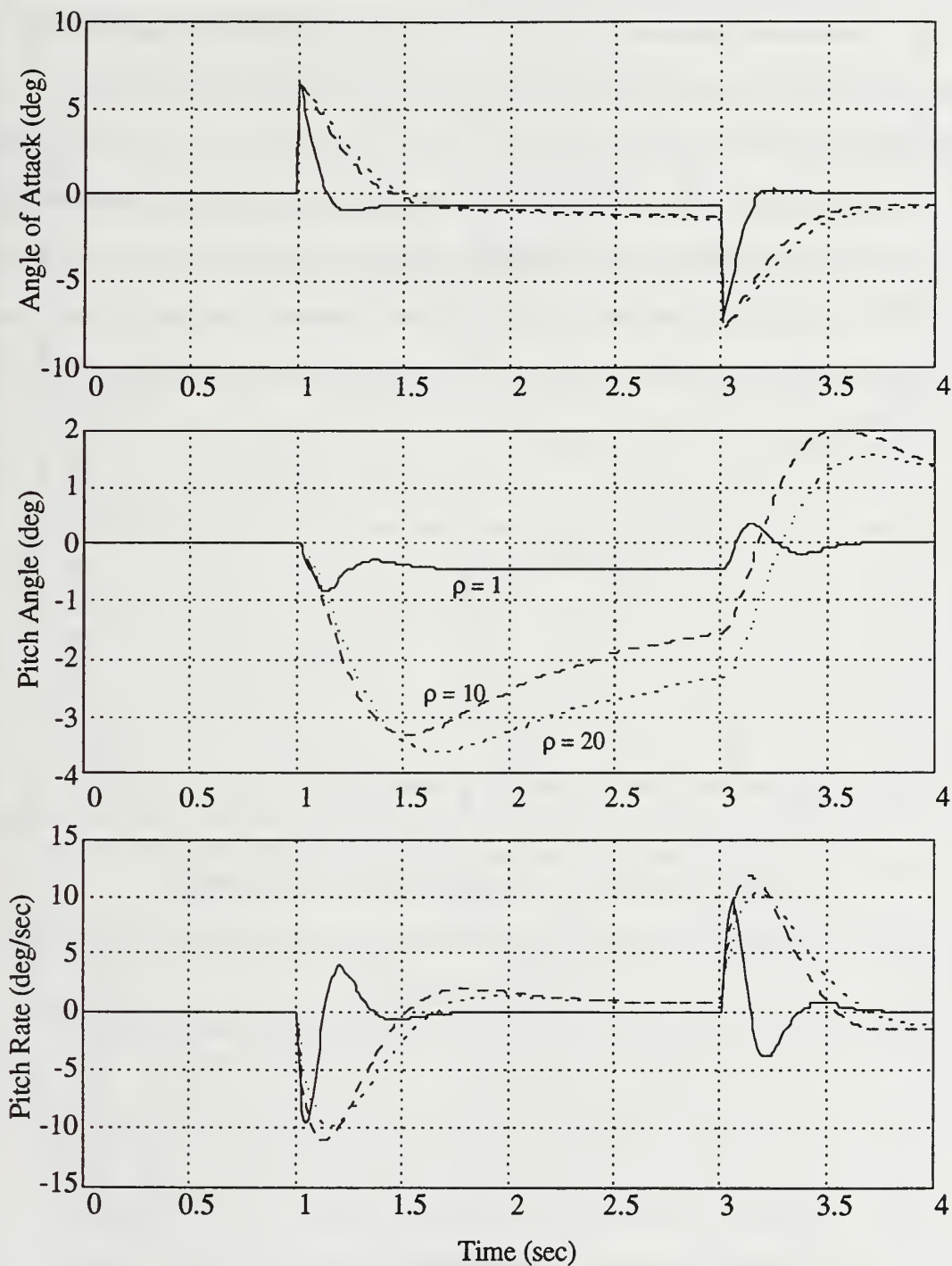


Figure 5.20 Rectangular Gust Response for
 $\tilde{R} = \rho R, \tilde{Q} = Q + (\rho - 1)SR^{-1}S^*, \rho \geq 1$

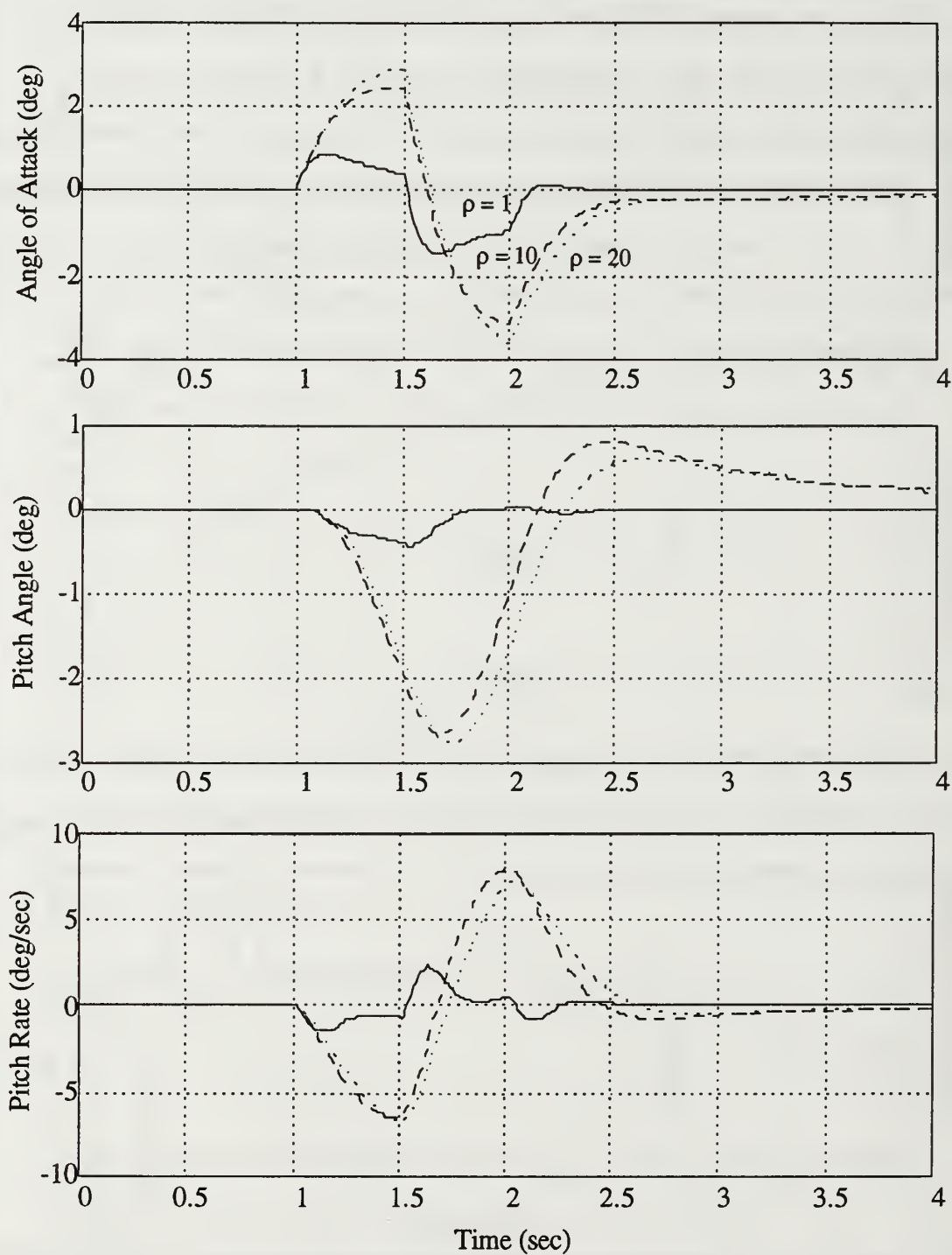


Figure 5.21 Triangular Gust Response for
 $\tilde{R} = \rho R, \tilde{Q} = Q + (\rho - 1)SR^{-1}S^*, \rho \geq 1$

6. System with $\tilde{Q} = \rho Q$

From Figures 5.22 and 5.23 it appears that the cost is increasing nearly linearly with ρ . However, for $1 \leq \rho \leq 5$ the robustness increases dramatically while the cost only goes up to about 25. This isn't as good as using option IV, where the cost increased far less for a comparable increase in robustness, but it does show increased robustness with a variable parameter. Figures 5.24 and

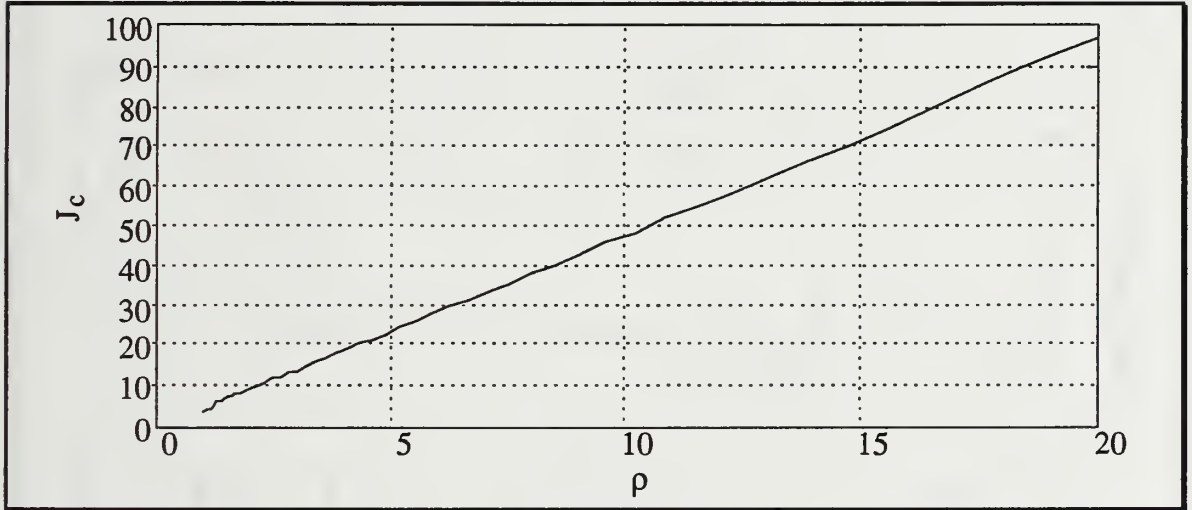


Figure 5.22 Performance vs ρ for $\tilde{Q} = \rho Q$

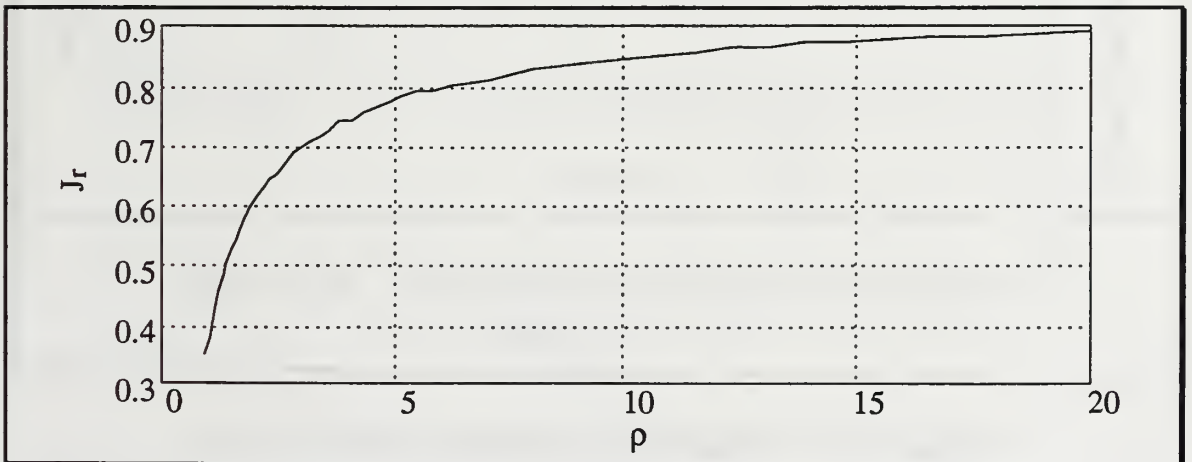


Figure 5.23 Robustness vs ρ for $\tilde{Q} = \rho Q$

5.25 show that the responses for both types of disturbance are still quite good.

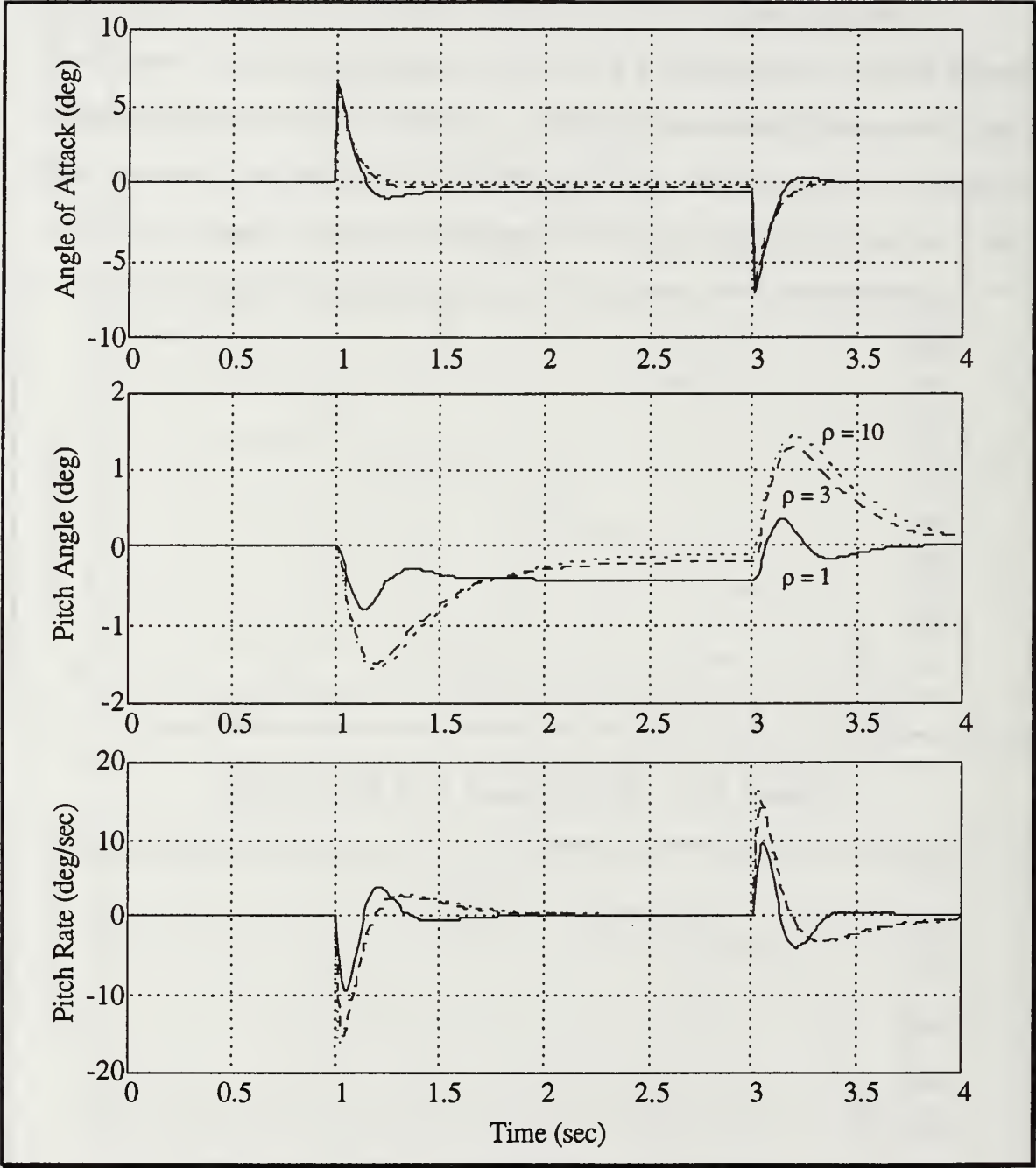


Figure 5.24 Square Gust Response for $\tilde{Q} = \rho Q$

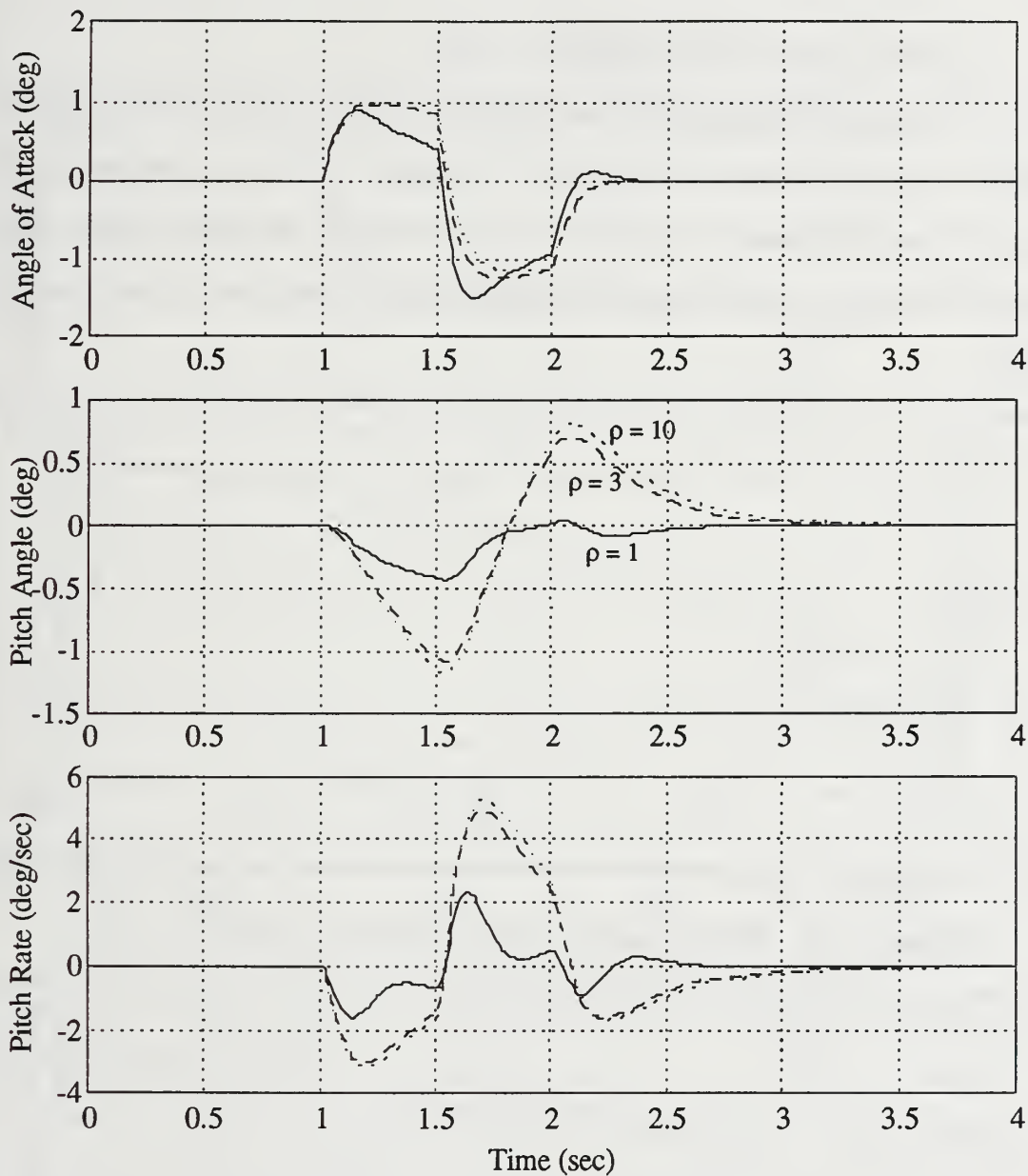


Figure 5.25 Triangular Gust Response for $\tilde{Q} = \rho Q$

7. System with $\tilde{Q} = Q + \rho SR^{-1}S^*$, $\rho \geq 1$

Figures 5.26 through 5.29 show that this option gives excellent results, similar to and slightly better than option IV. Using $\rho = 10$ gives a robustness of nearly 0.8 and increases the cost to only about 11.7. It would appear that options IV and VII would be the best choices for suboptimal robust control design.

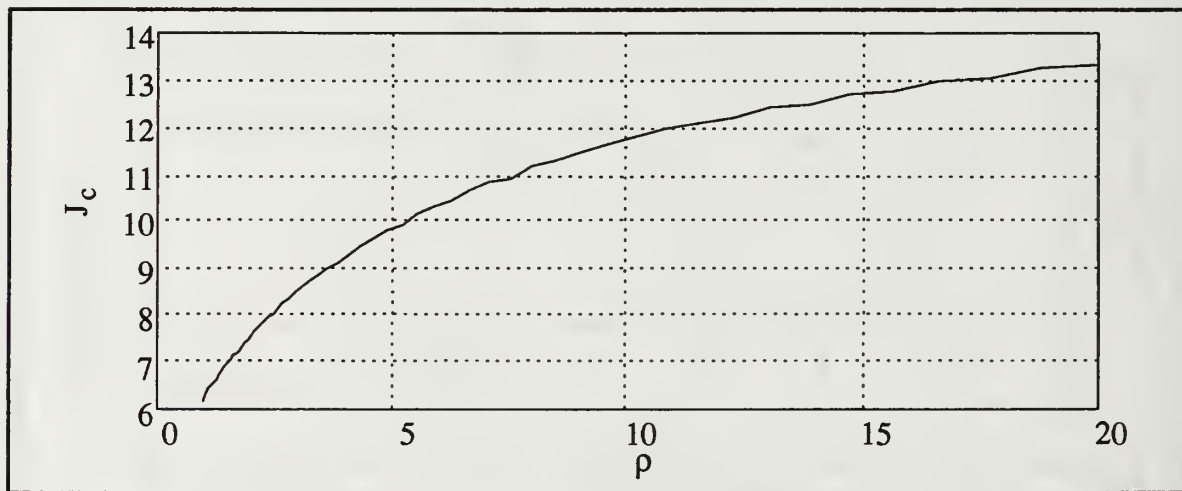


Figure 5.26 Performance vs ρ for $\tilde{Q} = Q + \rho SR^{-1}S^*$, $\rho \geq 1$

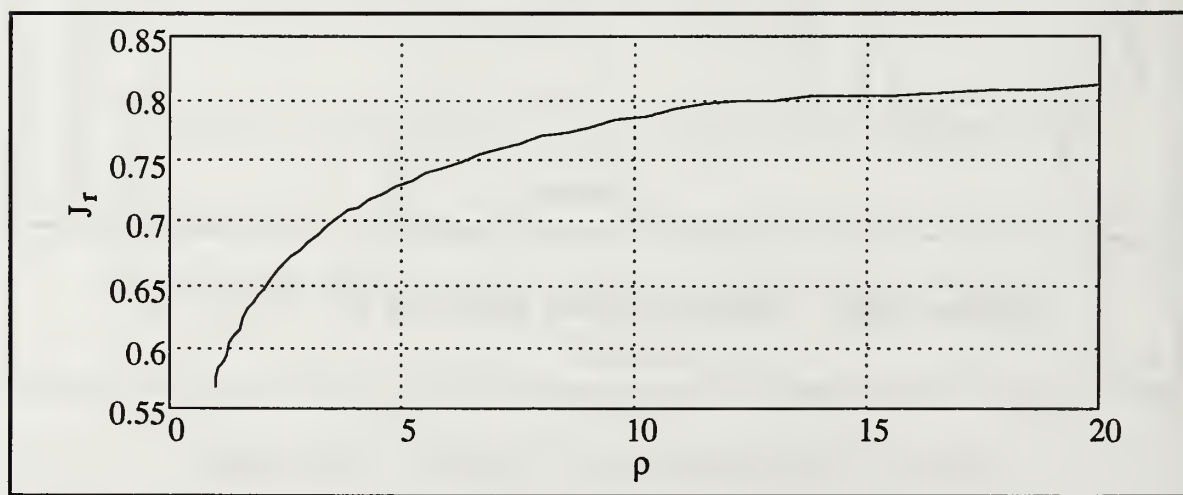


Figure 5.27 Robustness vs ρ for $\tilde{Q} = Q + \rho SR^{-1}S^*$, $\rho \geq 1$

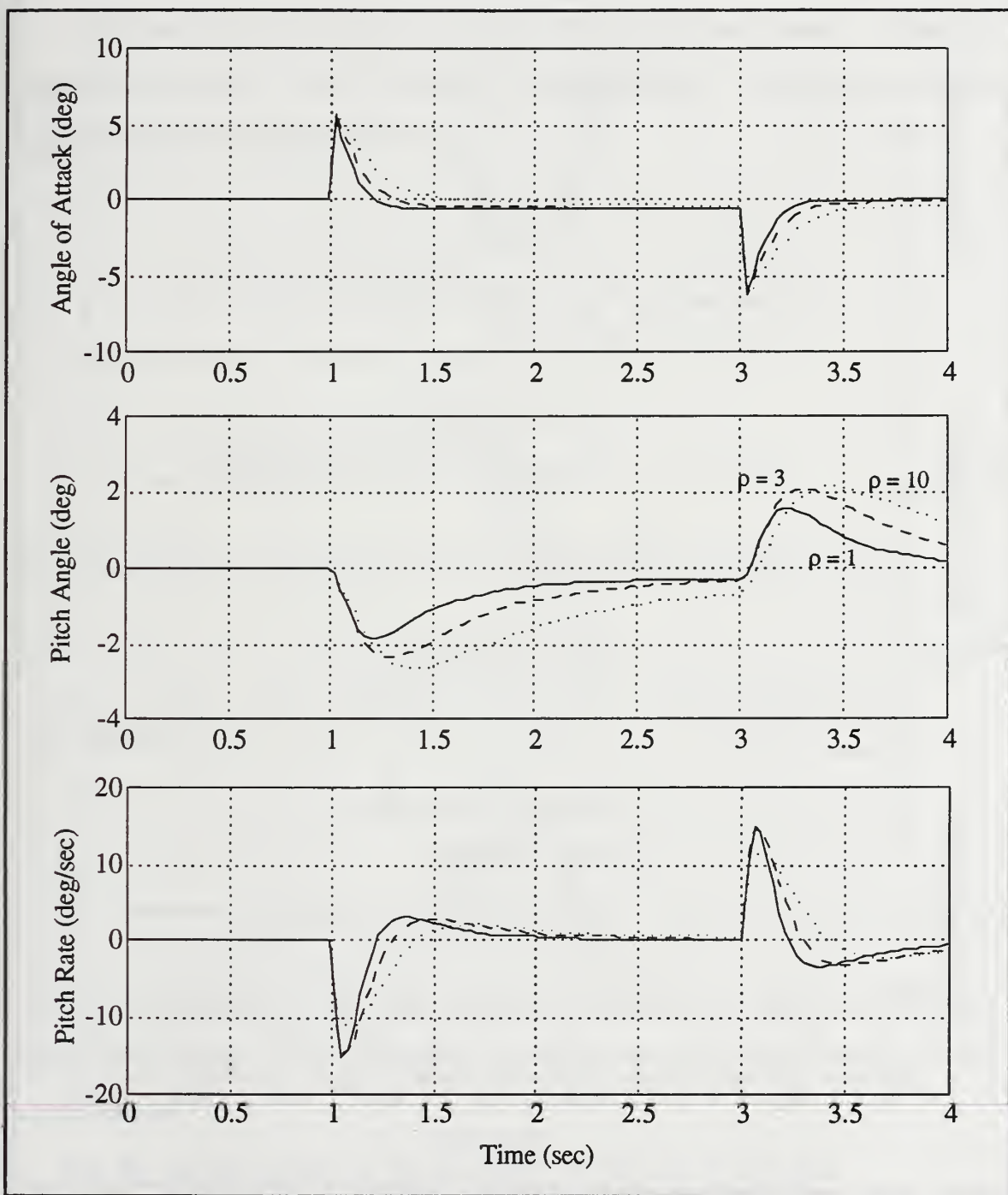


Figure 5.28 Square Gust Response for $\tilde{Q} = Q + \rho SR^{-1} S^*$, $\rho \geq 1$

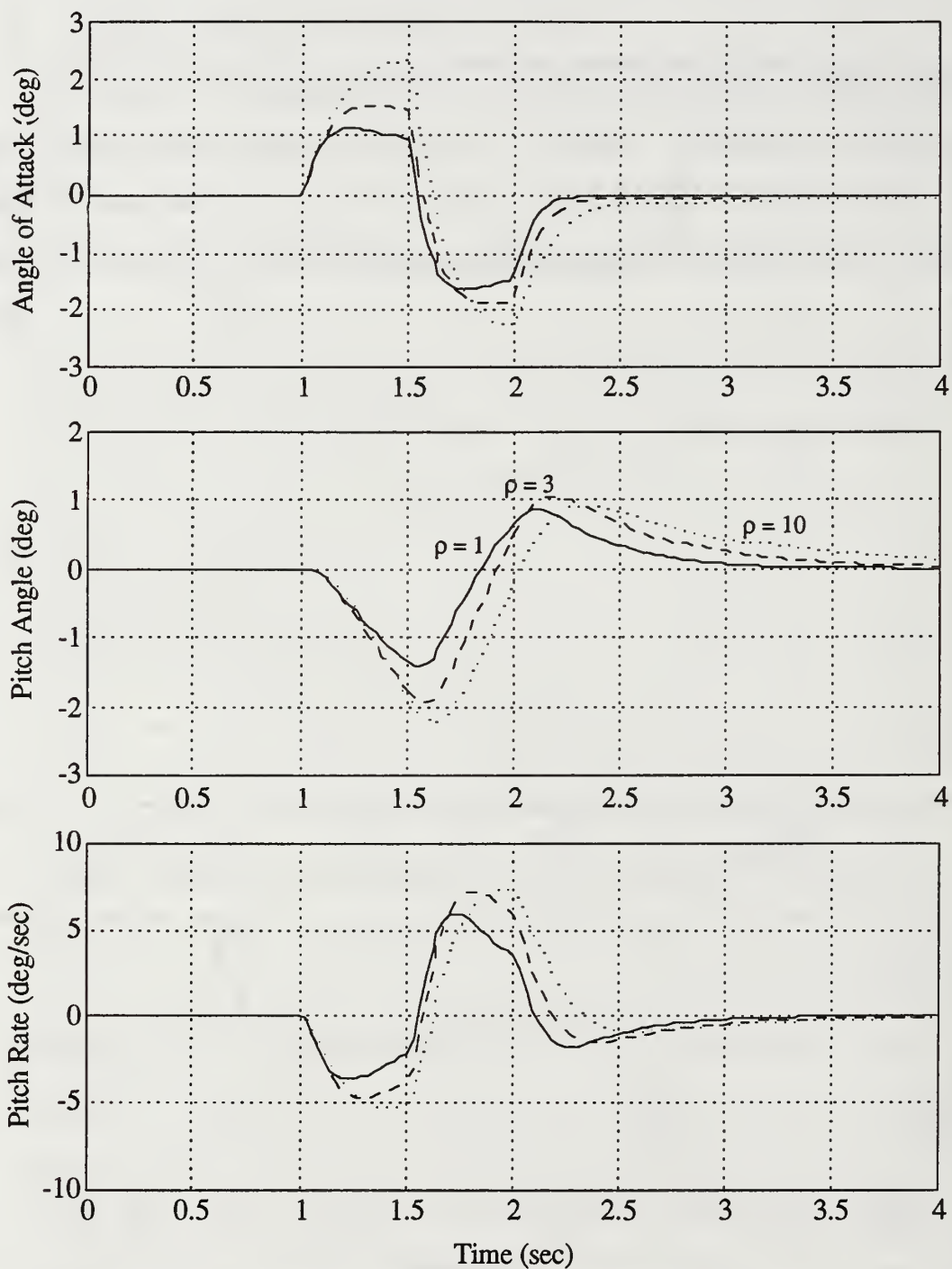


Figure 5.29 Triangular Gust Response for $\tilde{Q} = Q + \rho SR^{-1} S^*$, $\rho \geq 1$

C. FURTHER INVESTIGATION OF OPTION IV

As shown in the previous section, this suboptimal design displayed significant promise. In this section, the effects of ρ are further studied. Equation (2-32) is repeated here:

$$J = \frac{1}{2} \int_{-\infty}^{\infty} (x^* \ z_1^* \ z_2^* \ u^*) \begin{bmatrix} \Gamma_1 & \Gamma_2 & 0 & 0 \\ \Gamma_2^* & \Gamma_3 & 0 & 0 \\ 0 & 0 & \Psi_1 & \Psi_2 \\ 0 & 0 & \Psi_2^* & \Psi_3 \end{bmatrix} \begin{pmatrix} x \\ z_1 \\ z_2 \\ u \end{pmatrix} d\omega$$

$$= \frac{1}{2} \int_{-\infty}^{\infty} (x^* \ z_1^* \ z_2^* \ u^*) \begin{bmatrix} Q & S \\ S^* & R \end{bmatrix} (x \ z_1 \ z_2 \ u)^T d\omega. \quad (5-15)$$

It is evident that multiplying S by ρ is in effect multiplying Ψ_2 by ρ . But,

$$\Psi_2 = N^* R_3 J + N^* R_2^*, \quad (5-16)$$

and therefore

$$\begin{aligned} \rho \Psi_2 &= \rho(N^* R_3 J + N^* R_2^*) \\ &= \rho N^* R_3 J + \rho N^* R_2^* \\ &= \tilde{N}^* R_3 J + \tilde{N}^* R_2^*. \end{aligned} \quad (5-17)$$

Since N is produced by the augmentation of the inputs as given in (2-28), the physical result then, is a modification of $\Pi(j\omega)$, the frequency shaping of the control inputs.

For the aircraft system in this example, (5-10) and (5-12) give

$$\begin{aligned} u_1 &= N z_1 + J \delta_h \\ &= -z_1 + \delta_h \end{aligned} \quad (5-18)$$

and

$$\begin{aligned} u_2 &= Nz_2 + J\delta_f \\ &= -z_2 + \delta_f. \end{aligned} \quad (5-19)$$

Working backwards through the augmentation procedure,

$$\begin{aligned} u_1 &= \left(J - \frac{30\tilde{N}}{s+30} \right) \delta_h \\ &= \left(\frac{(s+30)J - 30\tilde{N}}{s+30} \right) \delta_h \\ &= \left(\frac{s+30-30(\rho)}{s+30} \right) \delta_h \end{aligned} \quad (5-20)$$

and

$$u_2 = \left(\frac{s+30-30(\rho)}{s+30} \right) \delta_f. \quad (5-21)$$

For $\rho = 1$, (5-20) and (5-21) reduce to the original high-pass filter and the resulting response and robustness are those of the optimal system. Decreasing ρ to -1 in several steps alters the frequency shaping as shown in Figure 5.30. Evidently, this aircraft system is more robust if low-pass filtering is used on the control inputs.

Another interesting point is that ρ had to be limited to $[-1, 1]$ for this system. Outside these limits, $\tilde{Q} = Q - SR^{-1}S^*$ was no longer positive semi-definite as required by optimal control theory to ensure a stable close-loop system.

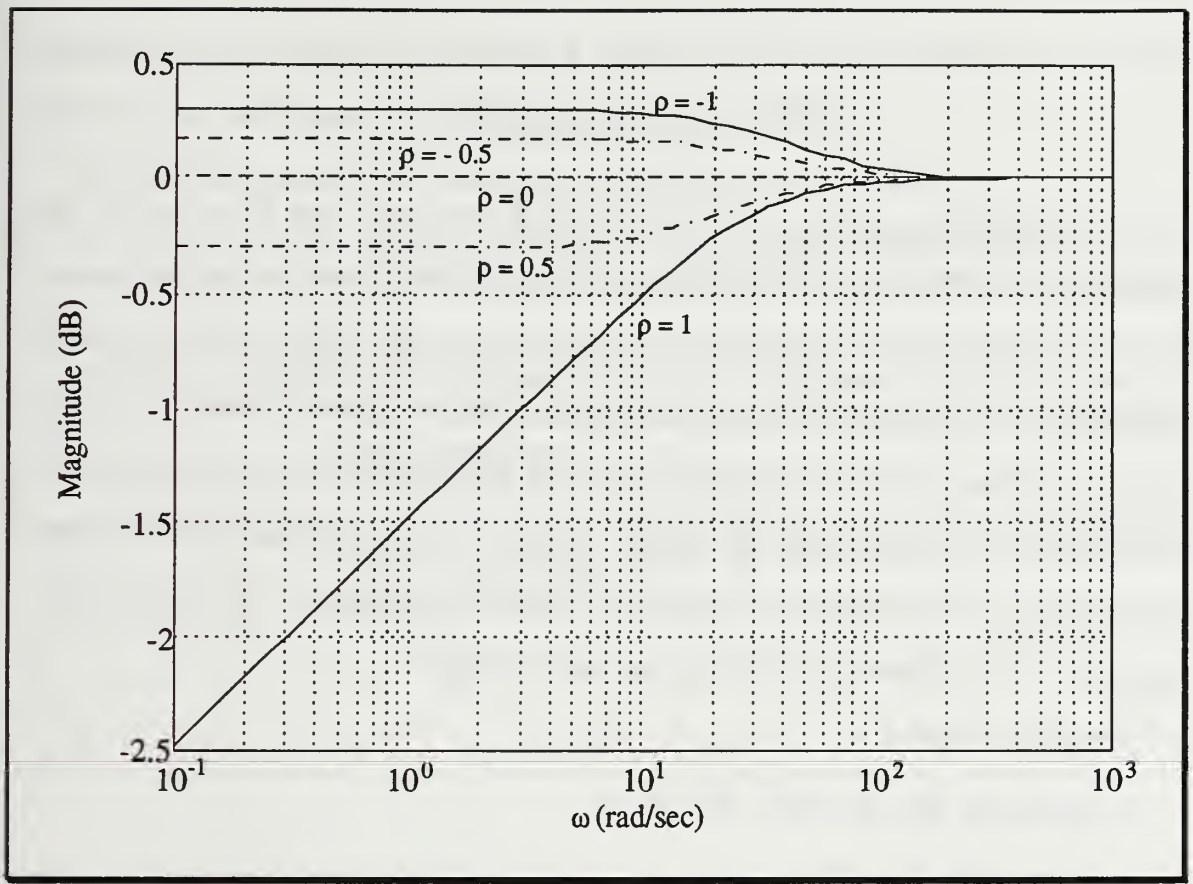


Figure 5.30 Frequency Shaping as a Function of ρ

VI. CONCLUSION

The frequency shaping in the generalized quadratic cost function can be converted to the standard linear quadratic control form by state augmentation. However, this process generates coupling between the states and the control inputs and eliminates the guaranteed good robustness characteristics of LQ optimal designs. This thesis has explored and developed a design technique for improving the robustness of these systems. This technique involves modification of the stability equations to regain robustness at the expense of optimality. The following modifications were studied:

- Option I: $\tilde{S} = 0$
- Option II: $\tilde{Q} = Q + SS^*$, $\tilde{R} = R + I$
- Option III: $\tilde{R} = \rho R$
- Option IV: $\tilde{S} = \rho S$, $\rho \leq 1$
- Option V: $\tilde{R} = \rho R$, $\tilde{Q} = Q + (\rho - 1)SR^{-1}S^*$, $\rho \geq 1$
- Option VI: $\tilde{Q} = \rho Q$
- Option VII: $\tilde{Q} = Q + \rho SR^{-1}S^*$, $\rho \geq 1$

All of these involve modifications to the weighting matrices in the cost function. The unstable aircraft model used in the simulations in this thesis responded best to Options IV and VII.

This thesis provides control systems designers with the ability to perform a trade-off between optimized performance and robustness. This is accomplished through the introduction of an adjustable parameter in the governing stability

equations. This approach provides a direct and straight-forward tool which designers can easily apply to their specific control problems.

In addition, some areas identified for future research include:

- Analysis of the physical meaning of the changes made by each of the design options, similar to that done in Chapter V for Option IV.
- More comprehensive comparison of all the options with each other to identify their similarities and differences in response for various values of ρ .
- Study of the effectiveness of this technique for systems in which observers or Kalman filters are necessary due to the use of partial state feedback.

REFERENCES

- [1] R. E. Kalman, "*Contributions to the Theory of Optimal Control*," Pol. Soc. Mat. Mex., Vol. 5, pp 102-119, 1960.
- [2] R. E. Kalman, "*When is a Linear System Optimal?*" Trans. ASME, J. Basic Eng., Vol. 86, pp 1-10, 1964.
- [3] W. Z. Chen, "*Constrained Optimization Approach to Feedback Control of State Augmented Systems*," Ph.D. Dissertation, University of California, Los Angeles, California, 1990.
- [4] W. Z. Chen, "*Parameter Optimization for an H_2 Problem with Multivariable Gain and Phase Margin Constraints*," presented at the American Controls Conference, Chicago, Illinois, 24-26 June 1992.
- [5] J. C. Doyle and G. Stein, "*Multivariable Feedback Design: Concepts for a Classical/Modern Synthesis*," IEEE Trans. on Automatic Control, Vol. AC-26, No. 1, pp 4-16, 1981.
- [6] I. Postlethwaite, J. M. Edmunds, A. G. J. MacFarlane, "*Principle Gains and Principle Phases in the Analysis of Linear Multivariable Feedback Systems*," IEEE Trans. on Automatic Control, Vol. AC-26, No. 1, pp 32-46, 1981.

INITIAL DISTRIBUTION LIST

	No. Copies
1. Defense Technical Information Center Cameron Station Alexandria, Virginia 22314-6145	2
2. Library, Code 52 Naval Postgraduate School Monterey, California 93943-5000	2
3. Chairman, Code EC Department of Electrical & Computer Engineering Naval Postgraduate School Monterey, California 93943-5000	1
4. Prof. Won-Zon Chen, Code EC/Cw Department of Electrical & Computer Engineering Naval Postgraduate School Monterey, California 93943-5000	1
5. Prof. Jeffrey B. Burl, Code EC/Bl Department of Electrical & Computer Engineering Naval Postgraduate School Monterey, California 93943-5000	1
6. Prof. George Thaler, Code EC/Tr Department of Electrical & Computer Engineering Naval Postgraduate School Monterey, California 93943-5000	1
7. Lt. Kurtis B. Miller Navy Undersea Warfare Center, New London Detachment New London, Connecticut 06320	2
8. Harold M. Miller 2314 Bennett Ave. Glenwood Springs, Colorado 81601	1
9. Kenneth E. Smith 109 Bluegrass Dr. Schererville, Indiana 46375	1

DUDLEY KNOX LIBRARY
NAVAL POSTGRADUATE SCHOOL
MONTEREY CA 93943-5101

DUDLEY KNOX LIBRARY



3 2768 00308606 7